UNIVERSITY OF CRETE

DEPARTMENT OF CHEMISTRY

GENERAL POSTGRADUATE PROGRAMME

MASTER THESIS

"Synthesis of biocompatible, pH-responsive and biodegradable polyesters"

STYLIANI AFRODITI MOUNTAKI

Supervisor: Professor MANOLIS STRATAKIS

HERAKLION 2021

ΠΑΝΕΠΙΣΤΗΜΙΟ ΚΡΗΤΗΣ

ΤΜΗΜΑ ΧΗΜΕΙΑΣ

ΠΡΟΓΡΑΜΜΑ ΜΕΤΑΠΤΥΧΙΑΚΩΝ ΣΠΟΥΔΩΝ ΣΤΗ ΧΗΜΕΙΑ

ΜΕΤΑΠΤΥΧΙΑΚΟ ΔΙΠΛΩΜΑ ΕΙΔΙΚΕΥΣΗΣ

«Σύνθεση βιοσυμβατών, pH-αποκρίσιμων και βιοδιασπώμενων πολυεστέρων»

ΣΤΥΛΙΑΝΗ ΑΦΡΟΔΙΤΗ ΜΟΥΝΤΑΚΗ

Υπεύθυνος Καθηγητής: Καθηγητής ΜΑΝΩΛΗΣ ΣΤΡΑΤΑΚΗΣ

ΗΡΑΚΛΕΙΟ 2021

ΕΞΕΤΑΣΤΙΚΗ ΕΠΙΤΡΟΠΗ

Μανώλης Στρατάκης

Καθηγητής, Τμ. Χημείας, Π.Κ.

Μαρία Βαμβακάκη

Καθηγήτρια, Τμ. Επιστήμης και Τεχνολογίας Υλικών, Π.Κ.

Μαρία Χατζηνικολαΐδου

Αναπληρώτρια Καθηγήτρια, Τμ. Επιστήμης και Τεχνολογίας Υλικών, Π.Κ.

ACKNOWLEDGMENTS

I would like to thank all the people that have supported me and helped με fulfill my master's thesis during these 2 years.

First and foremost, I would like to give special thanks and appreciation to my supervisor, Professor Maria Vamvakaki, for providing me with the chance to complete my master's thesis in the Material's Chemistry Lab. I want to thank her for her guidance, advice and the opportunity to learn more about polymers throughout these years. I would also like to thank Associate Professor Maria Chatzinikolaidou for the excellent collaboration during my thesis project and while using the lab's facilities and 3D-printer, and Professor Manolis Stratakis for his willingness to be the supervisor of my master's.

I would also like to express my gratitude to Dr. Maria Kalyva for the collaboration, for her guidance, understanding and for all the things I have learned from her in the lab through this time.

I would also like to thank the PhD candidate Konstantinos Loukelis, for performing all the biological experiments and for helping me with the 3D-printer's operation.

I want to thank my colleagues at the polymer lab, Dr. Theodoros Manouras, Dr. Eva Vasilaki, PhD cand. Maria Psarrou, and the rest of the lab members Maria, Dimitris G., Nikos, Giorgos, Dimitra, Anna, Dimitris F. Maya, Ioanna, Vasilis, Sylwia, Gabriella and Irene for their support and their collaboration in the lab.

A huge thank you goes to my friends outside the lab for always understanding and supporting me.

I could not thank enough my parents, Giorgos and Maria and my brothers, Kostas and Dimitris for supporting and encouraging me every day all these years.

Finally, the biggest thank you goes to Meletis, who stood by me from the begging of my academic adventure and always believed in my capabilities even when I didn't.

Thank you all!!!

Abstract

Aliphatic polyesters have been extensively used in the biomedical field, for tissue engineering applications. Despite their numerous benefits, such as biocompatibility and biodegradability, these materials are mostly inert and lack specific functionalities that would provide them with extra biological and responsive characteristics, such as pH, temperature, mechanical stimuli etc., whereas the synthetic route followed usually requires multistep synthesis with strict conditions.

In this work, pH-responsive aliphatic polyesters have been prepared by a facile condensation polymerization of a vinyl functionalized diol with a diacid chloride, followed by a carboxylic acid-functionalization along the polymer chains, via a photo-induced thiol-ene click reaction. The post-synthesis functionalization was conducted using two different mercaptocarboxylic acids, namely 3-mercaptopropionic and thioglycolic acid allowing the variation of the alkyl chain length of the side pendant groups. Furthermore, by adjusting the irradiation period during the click reaction, the degree of modification, and hence the carboxylic acid content of the polymers, could be easily controlled. Both of these characteristics were shown to have a significant impact on the responsive behavior of the polyesters with adjustable pKa values and water solubilities. To assess the biological properties of the materials in vitro, thin film of the difunctional polyesters bearing both alkene and carboxylic acid moieties were prepared by chemically linking the pendant vinyl bonds of a silanized substrate with the polymers' side groups. The polymeric thin films with the shorter alkyl chain and the highest functionalization degree (PE-Glyc50) were found to promote greatly the cell viability, proliferation, and attachment when assessed in L929 fibroblast cultures. Next the PE-Glyc50 polyester, as well as a blend of the same polyester with laponite, were blended with PEGDMA as the crosslinker, to develop stable 3D scaffolds via an extrusion-based printing method. Finally, the optimized printing conditions resulted in structures that were investigated for their degradability and the influence of the pH on their swelling behavior, porosity.

Table of Contents

Abbreviations

TE	Tissue engineering
3D	Three dimensional
ECM	Extracellular matrix
HA	Hydroxyapatite
ESB	European society of biomaterials
SEC	Size exclusion chromatography
GPC	Gel permeation chromatography
NMR	Nuclear magnetic resonance
ATR – FTIR	Attenuated total reflectance – Fourier transform infrared
TGA	Thermogravimetric analysis
DSC	Differential scanning calorimetry
WCA	Water contact angle
UV-Vis	Ultraviolet-visible
SEM	Scanning electron microscopy
THF	tetrahydrofuran
TEA	triethylamine
ADC	adipoyl chloride
TPAE	trimethylolpropane allyl ether
DCM	dichloromethane
DMF	dimethylformamide
DMPA	2,2-dimethoxy-2-phenylacetophenone
MAPTMS	3-(trimethoxysilyl)propyl methacrylate
$CHCl_3$	Chloroform
FBS	Fetal bovine serum
TCPS	Tissue culture polystyrene
DTT	dithiothreitol
PEGDMA	Poly(ethylene glycol) dimethacrylate

Chapter 1

1. Introduction

1.1 Tissue Engineering

Tissue and organ failure caused by disease, injury or developmental defects, has led to the emergence of tissue engineering (TE). TE is a relatively novel and interdisciplinary concept that is growing fast due to the limited availability of donated organs intended for transplantation, as well as the ever-increasing aging population. It is considered interdisciplinary, because it combines the principles of engineering and life sciences, to develop substitutes used to restore, maintain or enhance human tissues and organs. TE envisages the production of functional organs, built from scratch in the laboratory, focusing on the elimination of the current drawbacks rising from organ replacement, such as poor biocompatibility, low biofunctionality and immune rejection.

To regenerate new tissues, a multistep process that combines different components is needed. The necessary components for TE applications, though not always simultaneously used, are cell sources, scaffold fabrication and growth factors[1]. Cultured cells are coaxed to grow, producing 3-dimensional (3D) tissues on bioactive scaffolds that provide the appropriate physical and chemical environment, whereas the function of growth factors is to facilitate and promote cells to regenerate new tissue.

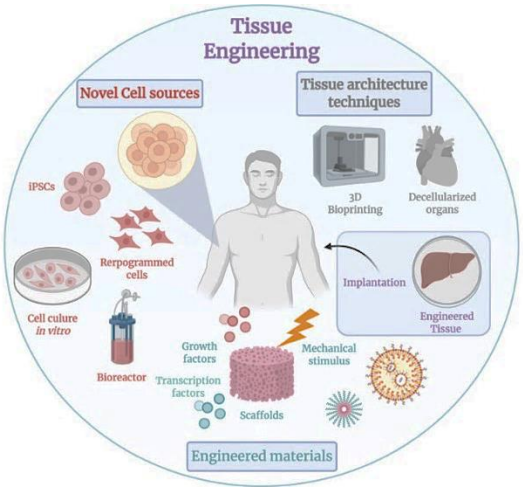

Figure 1: Key components in tissue engineering[41].

The choice of the cell source is a crucial aspect in designing and further developing the tissue engineered model. Cells derived from living species can be classified into autologous (from the same patient), allogenic (for other human donor) and xenogenic (from different species). Autologous cells are considered more suitable for TE, since they are highly bioactive and not immunogenic, in contrast to the allogeneic and xenogenic cells that require complementary immunosuppressive therapy. One downside of autologous cells' harvesting, is meeting the sufficient quantity, especially from senior or severely diseased patients. Allogeneic cells have been successfully used in diabetes, liver diseases and skin conditions such as ulcers, where they were engineered to develop FDA-approved skin patches[2]. Xenogenic are the least frequently utilized cells, since their use remains controversial, due to the possibility of transmitting animal pathogens to humans. Nonetheless, they can be used as a temporary solution, while the tissue repairs itself or until a human organ from a donor is available.

For most tissues and organs, unfortunately cells alone are not enough, otherwise a simple cell injection to the target site would be sufficient for tissue regeneration. The necessary support is provided by 3D scaffolds that have similar function as the extracellular matrix (ECM). These scaffolds should meet certain criteria to assist cell proliferation, differentiation and biosynthesis. Having interconnected micropores to facilitate the seeding of numerous cells and increase their number as well as the supply of nutrients, is one of these criteria. A pore size from 100 to 500 μm is considered optimal, as it can promote vascular formation and waste transport. Furthermore, a scaffold should have suitable mechanical properties and absorption kinetics to the surrounding tissue. For instance, the degradation rate should be slow in scaffolds intended for bone TE, to maintain mechanical support until the tissue is fully regenerated, whereas in skin TE the scaffold's fast degradation is preferred. The material's surface is also very important in regulating cell behavior, since it is the primary contact for cell interactions[3]. Several materials can be used as scaffolds, such as natural materials (i.e. collagen, fibrin, etc.), synthetic polymers (i.e. polyglycolide, polylactide, etc.), inorganic materials (i.e. hydroxyapatite, tricalcium phosphate, etc.) and composites (i.e. polylactide-hydroxyapatite, etc.).

Mimicking the local cellular microenvironment would include suitable physicochemical and biochemical factors to provide the appropriate signals that can launch the cascade of the healing process. Such factors can be proteins or signaling molecules which can inhibit or stimulate cellular proliferation, differentiation, migration, adhesion and gene expression. Their action is initiated

when they bind to specific receptors on the cell surface. They can be secreted by cells themselves or as a result of communicating cells. Moreover, different cell types can produce the same growth factors and different growth factors can affect different cells[4]. The most frequently used growth factors are the bone morphogenetic proteins (BMPs), the basic fibroblast growth factor (bFGF) and the vascular epithelial growth factor and transforming growth factor-b (TGF-b).

So far, TE has been applied to research concerning skeletal, cardiovascular, nerve and spinal cord systems, while clinical studies have already been conducted for skin, articular cartilage, urethra, bladder and myocardiac tissue with promising results. Of course, there are many challenges that researchers need to overcome, nonetheless, technological advances such as the use of stem cells, gene editing, 3D bioprinting and nanotechnology can expedite the fabrication of tissues destined for regenerative therapies that are patient-specific.

1.1.1 Bone Tissue Engineering

Bone tissue is a dynamic system that is essential for bodily locomotion, has load-bearing capacity and is providing protection of the delicate internal organs. Additionally, bones are involved in the organism's homeostasis by regulating the calcium and phosphate ion storage and can entrap dangerous metals like lead.

It is a dynamic tissue, both structurally and functionally, and its properties vary depending on the loading conditions, differentiating them to short (i.e. phalanges, etc.), long (i.e. tibia, etc.), flat (i.e. skull, etc.) and irregular (i.e. vertebrae, etc.)[5]. It is also arranged either in a compact pattern (cortical bone) or a trabecular pattern (cancellous bone). Bone tissue is organized hierarchically, with length scales varying from the macro – to the nanoscale (ECM components) (Figure 2). The bone nanostructure consists of collagen fibers, reinforced by hydroxyapatite (HA) crystals, which impart its tough and simultaneously flexible character. In addition, bone ECM is comprised by a plethora of non – collagenous proteins (i.e. glycoproteins, proteoglycans, etc.). On the macroscale, bones form many Harvesian canals that surround blood vessels and nerves, called osteons, which in turn are covered by an outer strong calcified compact layer[6].

Bone defects, up to a critical size, can be healed without external intervention, but when the trauma exceeds this size, invasive treatment is necessary. Current clinical treatments that focus on the regeneration of the tissue, among others include, autologous and allogeneic bone grafts.

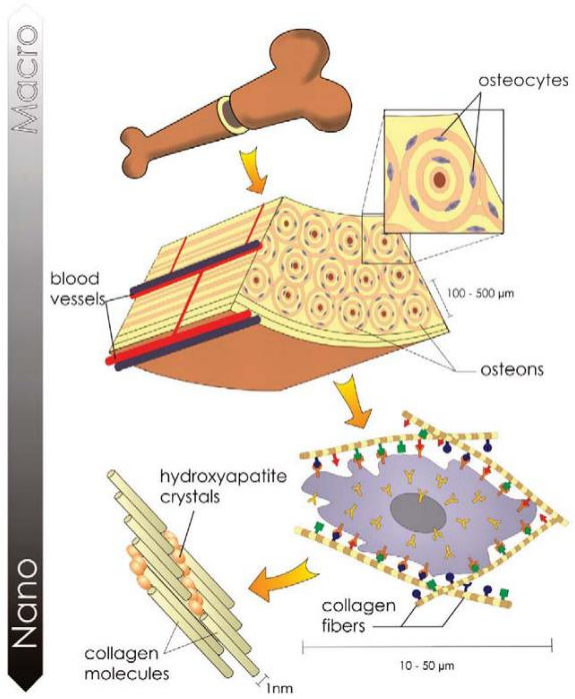

Figure 2: Schematic representation of the bone hierarchical organization[6].

Autografts, being histocompatible and non-immunogenic, can achieve osteoinduction (capability of promoting the differentiation of progenitor cells down an osteoblastic lineage), osteoconduction (support bone growth and encourage the ingrowth of surrounding bone) and osteointegration (integrate into surrounding bone). However, autografts require a second operation for the harvesting of the graft, which entails further surgical risk, like bleeding, inflammation and chronic pain. On the other hand, allografts, usually derived from a cadaver, are available in various forms, including demineralized bone matrix, whole bone segments, etc., but have reduced osteoinductivity and high risk of immunoreactions and infections.

During the last decades, there has been increased research on alternative treatment options using substitute materials that would, at best, eliminate the aforementioned complications. These materials include bioactive ceramics and glasses, natural or synthetic polymers and their composites. Ideally, upon implantation, they could induce tissue repair by releasing factors that promote it, and would be resorbed over time, leaving behind the body's own regenerated tissue.

1.2 Biomaterials and Scaffolds

According to the European Society of Biomaterials (ESB), a biomaterial is a "material intended to interface with biological systems to evaluate, treat, augment or replace any tissue, organ or function of the body". As expected, the field of TE relies on scaffolds comprised of biomaterials, to provide a microenvironment, where the cells will attach, proliferate, differentiate and eventually generate new tissue. These scaffolds, patterned in two- and three-dimensions, are usually seeded with cells, and occasionally other factors, and serve as biomimetic matrices, destined to generate complex tissue architectures. Essentially they act as templates aiming to facilitate and promote cellular responses that might not be normally present[7].

The last few decades, an abundance of scaffolds derived from a plethora of biomaterials, have been studied and produced with a great variety of techniques. When designing a scaffold and its properties, certain requirements should be met, regardless the tissue type it is intended for. First, the scaffold should be biocompatible. It must promote cell adhesion, normal function and proliferation, with a negligible immune reaction, to avoid causing a severe inflammatory response. Secondly, since scaffolds for TE applications remain temporarily on site, degradation is crucial to allow tissue formation. Depending on the tissue that the scaffold is designed for, it should have a fast or slow biodegradability rate and the by-products should be non-toxic and exit the body without any interference with other organs. Another criterion, is the mechanical properties, which should be compatible with the surrounding tissue, the patient's age. The scaffolds should also keep its integrity until the restoration completion and should withstand surgical handling. Another important consideration when determining a scaffold's suitability for the target tissue, is its architecture. As already mentioned above, scaffolds should have interconnected pores to maximize the cell penetration and ultimately proliferation, as well as to allow nutrient diffusion and waste disposal. Additionally, on the practical side, scaffolds must be cost-effective and easily scalable, ensuring the successful availability to the clinician. Lastly, the choice of the biomaterial the scaffold is comprised of, is of the utmost importance. Usually there are five types of biomaterials used in TE, namely natural polymers, synthetic polymers, ceramics, metals and composites. Each type of biomaterial has both advantages and disadvantages which are further discussed below[8].

1.2.1 Natural Polymers

TE has shown an increasing demand for natural polymers such as proteins, nucleic acids, polysaccharides, lipids and complex macromolecules, over the last years. Natural polymers have many advantageous properties because of their inherent biocompatibility and bioactivity. They can be easily processed and they mimic the natural ECM of tissues[9], while promoting excellent cell adhesion and growth, due to their binding sites (RGD motifs). They can be mammalian (i.e. collagen, elastin, hyaluronic acid, etc.) and non-mammalian (i.e. alginate, dextran, chitosan, etc.) derived, making them a cheap and commercially available biomaterial. Natural polymers can also be stabilized into scaffolds through either self-assembly or by crosslinking techniques, imitating the natural tissue. However, fabricating scaffolds from biological materials with homogeneous and reproducible properties can be challenging, due to natural variability in the *in vivo* source. Additionally, the scaffolds show poor mechanical properties, fast biodegradability and the potential impurities may result in unwanted immune reaction[10].

1.2.2 Synthetic Polymers

To overcome the natural polymers' disadvantages, numerous synthetic polymers have been studied. Synthetic polymers can have tailor-made shapes, architectures, chemistry and functions, aiming to serve as bioactive matrices and templates that mimic the ECM systems. These materials can be produced in various forms and offer great reproducibility, on demand availability, and control over their mechanical modulus and tensile strength, as well as their degradation rate. Some of the most widely used polymeric materials are polylactic acid (PLA), poly(ethylene glycol) (PEG) and poly(ε-caprolactone) (PCL), which are biocompatible, biodegradable and in the case of the former two, FDA-approved. At first, those polymers were utilized as sutures, but during the years their application range has expanded to TE scaffolds (i.e. urethral tissue, etc.) and drug delivery systems (i.e. stem cell delivery, etc). Nevertheless, synthetic polymers lack sites for cell adhesion and the biocompatibility is often questionable, since many degradation products can be cytotoxic.

1.2.3 Ceramics

Ceramic biomaterials or bioceramics, are refractory and polycrystalline compounds, used in biological applications. They are often derived from inorganic materials, such as calcium, silica, phosphorous, magnesium, potassium, and sodium, sintered or melted to create porous scaffolds. According to the type of host-tissue interactions, they can be classified as bioinert or bioactive, and the bioactive ones can be further categorized as resorbable and non-resorbable. Bioceramics, such as, alumina (Al_2O_3), zirconia (ZrO_2) and hydroxyapatite ($Ca_{10}(PO_{46}(OH)_2)$), have been extensively studied for skeletal system applications, including bone, joint and teeth implants. Some of their major appealing characteristics as implants are their inertness, hardness, thermal and electrical properties, high compressive strength and biocompatibility. However, their advantages as implants can turn into disadvantages for TE applications, for example, because of their brittleness and difficulty of shaping, clinical applications are currently limited[11].

Table 1: Summary of mechanical properties of various bioceramics.

Materials	Density ($g\,cm^{-3}$)	Hardness (Vickers, HV)	Young's modulus (GPa)	Bending strength (MPa)	Compressive strength (MPa)	Fracture toughness K_{IC} ($MPa\,m^{1/2}$)
Bioglass® 45S5	2.66	458	35	40–60		0.4–0.6
A-W glass-ceramic	3.07	680	118	215	1080	2.0
Bioverit glass-ceramic	2.8	5000	70–88	140–180	500	1.2–2.1
Sintered HA	3.156	500–800	70–120	20–80	100–900	0.9–1.3
Alumina	3.98	2400	380–420	595	4000–4500	4–6
Zirconia (TZP)	6.05	1200	150	1000	2000	7
Zirconia (Mg-PSZ)	5.72	1120	208	800	1850	8
316 stainless steel	8		200	540–1000*		~100

* = tensile strength.

1.2.4 Metals

Metals such as stainless steel, cobalt and titanium alloys have been extensively used as implants and scaffolds, because of their good mechanical properties, including high elastic modulus, yield strength and high ductility, which allow them to withstand load pressure without distorting. However, there are significant limitations in their employment in TE applications, as they tend to show lower surface cell adherence. Furthermore, metal scaffolds can be corrosive in biological fluids, which can lead to the alteration of their surface properties, as well as the release of toxic metal ions as byproducts[12].

1.2.5 Composites

As already mentioned above, all types of biomaterials can have disadvantages. Combining two or more different biomaterials with notably different chemical or physical properties, such as synthetic polymers and bioceramics, can help overcome the drawbacks or shortcomings emerging from each material and can help create a scaffold with unique properties.

1.3 Aliphatic Polyesters in Tissue Engineering

Aliphatic polyesters are among the most frequently utilized biodegradable polymers in biomedical and TE applications and have been widely investigated in the past years. Ester linkages are very common in nature, therefore, it would be expected that synthetic polymers containing such bonds would exhibit degradable behavior[13]. Indeed, some of the most well-known aliphatic polyesters, i.e. polylactide (PLA), polycaprolactone (PCL) and polyglycolide, have found many applications as biodegradable biomaterials in drug delivery and TE due to their ability to biodegrade in the presence of cells and tissues[14,15]. Aliphatic polyesters degrade primarily by the hydrolysis of their main chain ester linkages, and the rate and degree of degradation are determined by the polymer's properties (i.e. hydrophilicity and crystallinity), whereas they deteriorate by either bulk or surface erosion[16].

Besides these prominent features, polyesters have some disadvantages, the most significant being their hydrophobicity and the lack of functional pendant groups along the polymer backbone. Functional pendant groups, like amine, hydroxyls and carboxylic acids can alter the physicochemical and biological characteristics of a biomaterial, influencing the cellular adhesion, proliferation and differentiation on biomaterial scaffolds[17]. Furthermore, cellular activity can be directed by conjugating bioactive compounds, such as proteins and peptides onto the polymer. Lastly, the addition of stimuli-responsive (i.e. pH, temperature, redox, light, etc.) functional groups can provide polymers with extraordinary qualities and tunable behavior[18]. Therefore, it is clear that developing materials with such properties can benefit the TE landscape.

1.3.1 Synthetic Approaches to Functional Aliphatic Polyesters

In the recent years, biodegradable aliphatic polyesters functionalized with side groups, have gained increasing interest. The most common approaches to synthesize such materials are, ring opening polymerization (ROP), polycondensation as well as post-polymerization functionalization.

ROP is the most common method used for the preparation of functional polyesters with high molecular weights and it can be implemented using a variety of methods, including anionic, cationic and enzymatic polymerization. A typical strategy to prepare polyesters by ROP, involves the polymerization of functional lactone and lactide monomers (Figure 3), using a wide variety of initiators, including organocatalysts, metal alkoxides, and various metal complexes[19]. Furthermore, O-carboxyanhydrides (OCAs) have emerged as an alternative class of highly active monomers for the synthesis of poly(α- hydroxy acids). Finally, the synthesis of functional polyesters via the radical ring-opening copolymerization of cyclic ketene acetals with conventional vinyl monomers was reported[20]. However, the aforementioned methods involve either a complex multistep synthetic route or a reaction performed under very strict conditions.

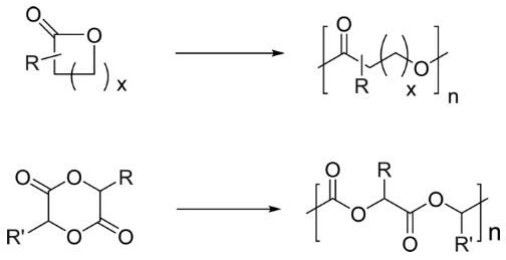

Figure 3: ROP of lactone (top) and lactide (bottom) monomers.

The second approach, the polycondensation or step-growth polymerization, refers to the condensation of hydroxy-acids or mixtures of diacids and diols. This method has been used to prepare polyesters bearing diverse functional moieties such as azide, hydroxyl, alkene, alkyne and phosphate groups. The main disadvantages of this approach are the high temperatures and extended reaction periods required, which may result in side reactions such as racemization. The molecular weight of the polymers usually reaches up to a few tens of thousands (Mn < 30 kDa),

because the deviation from the 1:1 stoichiometry of the diacid and diol can detrimentally affect the chain length.

The final approach involves the post-polymerization functionalization of polyesters, by abstracting protons by base-treatment and by the subsequent addition of an electrophilic reagent (halogen- or carbonyl-containing compound). This method introduces a high risk of unwanted reactions, such as racemization and chain scission. Alternatively, a homopolymerization or copolymerization of functional monomers bearing functional side groups (i.e. alkenes, diisocyanates, thiols, etc.) can be performed to introduce functional moieties along the polyester chains.

1.4 Biofabrication Techniques

1.4.1 Conventional Biofabrication Techniques

Several techniques are used for the processing of synthetic and natural biomaterials into cell scaffolds. Some of the most common and conventional approaches are the following.

i. Solvent-casting and particulate-leaching: In this method, a polymer solution is uniformly mixed with salt particles in a solvent. The solvent is left to evaporate leaving behind a polymer matrix embedded with salt particles. When the matrix is immersed in water, the salt particles are dissolved, leaving behind a porous structure[21].

ii. Freeze-drying: In freeze-drying, or lyophilization, the polymer solution is cooled down below the freezing point of the solvent, and subsequently is subjected to vacuum drying that causes the sublimation of the solvent, resulting in porous materials[22].

iii. Electrospinning: This technique exploits the electrostatic forces developed between a feeding capillary tube and a metal collector. When high voltage is applied, the polarity created accelerates a string of the polymer from the tube towards the collector, creating a mat of nano- or micro-fibers[23].

Other common techniques for biofabrication, include gas foaming, phase separation, melt molding, etc.

1.4.2 Additive Manufacturing (AM)

Additive manufacturing or 3D-printing includes many different techniques to fabricate structures from a bottom-up approach and it has been employed extensively in TE and drug delivery. AM approaches use computer-aided (CADs) designs to create structures or patterns in a predefined manner. The CADs can geometrically be patient specific and have macro- and microarchitecture that corresponds to the anatomical properties of the target tissue. The most common AM methods are described below (Figure 4).

i. Extrusion printing: This technique is the most commonly used and includes the extrusion of a material filament onto a printing surface through a nozzle. The driving force that controls the extrusion is powered by a piston, a screw or is pneumatic-based. This method offers fast fabrication, but poor printing resolution (20 – 200 μm), which can be affected by the geometry of the nozzle and the shear stresses applied during the printing. Extrusion printing is compatible with hydrogels, as they are soft enough to be extruded or can be printed as a pre-crosslinked precursor and then stabilized post-printing by secondary crosslinking. Overall, it is considered a good printing method for complex structures at clinically relevant sizes and it provides versatility over the biomaterials that can be used[24].

ii. Inkjet printing: Inkjet printing is a cost-effective and simple technique. It works in the same way as an inkjet office printer, that is, the material droplets are discharged from a cartridge as a result of pressure created inside the nozzle by the development and rupture of microbubbles. The ejection of each droplet is caused by either piezoelectric or thermal stimuli. In the case of thermal stimulus, an air bubble is nucleated within the printhead by a heat source, causing a pressure rise and eventually droplet ejection. In the case of piezoelectric printers, an acoustic wave is used to drive the extrusion. Inkjet inks should be non-viscous, to ensure that they can be properly deposited and to minimize the shear forces experienced by cells as they exit the nozzle in the case of bioprinting. Furthermore, secondary crosslinking, after the deposition of the droplets, is required so that the printed construct can have more than one levels[25].

iii. Stereolithography: Stereolithography uses light-induced polymerization to produce 3D-printed structures that immerge from a tank of photosensitive resin. A beam of UV or visible light is directed at the resin, layer by layer or by a patterned structure and crosslinking takes place because of the radical-generating species (photoinitiator) present

in the resin. The platform moves on the z-axis to allow the unreacted monomers to polymerize. This method offers high resolution structures, but has a limited range of materials since they must be photosensitive[26].

Other AM techniques include selective laser sintering, laser assisted bioprinting, multi-photon polymerization, etc.

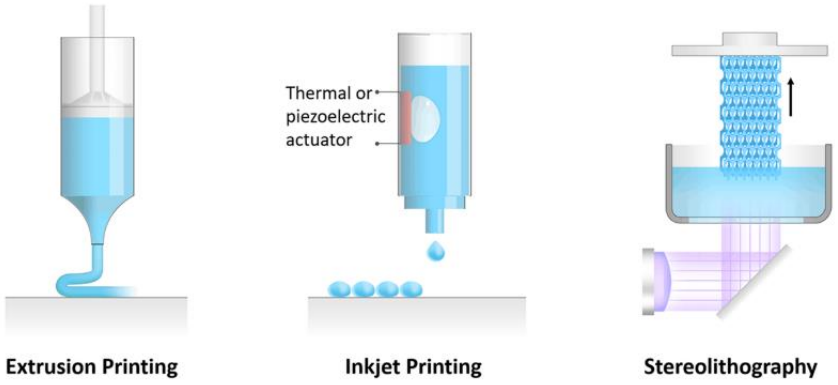

Figure 4: The most common additive manufacturing techniques[24].

1.5 3D Printing of Hydrogels

Hydrogels are water-swollen polymer networks formed by crosslinked polymer chains. Hydrogels can be classified into natural, synthetic and semi-synthetic in terms of the materials they are derived from. Hydrogels that remain physico-chemically stable and do not disintegrate into oligomers in a biological environment, are considered durable. In the recent decades, smart hydrogels have been produced, with the ability to respond when certain stimuli, such as pH, temperature, etc., are applied. Because of their soft and rubbery nature, which is comparable to that of the ECM, they have been studied extensively for TE applications, showing great *in vivo* biocompatibility and biodegradation[12].

Due to the limitations of the typical manufacturing techniques, hydrogels can only be formed into 2D or basic 3D structures through templating, which has led to an increasing scientific attention for the development of patterned hydrogels from the microscale to the macroscale. As already mentioned above, the 3D printing technology, which does not require molds, dies, or masks,

enables the quick transformation of digital designs into complex 3D structures on demand. Furthermore, several 3D printing methods that have been developed in the recent years, which are suitable for viscoelastic materials such as hydrogels[27]. Whether or not, a hydrogel qualifies for a certain 3D printing method, it solely depends on its physicochemical properties. More specifically, the printability of a hydrogel is determined by its rheological properties (viscosity, shear thinning, and yield stress) and the cross-linking mechanisms (physical or chemical). The viscosity of a polymeric solution or blended paste, such as a hydrogel precursor, is primarily determined by the polymer/precursor concentration and molecular weight in solution. For physically-crosslinked hydrogels, the crosslinking can occur both during and after the printing, whereas for the chemically-crosslinked ones, the crosslinking can happen at will, allowing the specific design of the hydrogel and its structure[28].

The latest advances in hydrogel 3D printing, include the introduction of a responsive behavior that has the ability to shape-shift the structure over time, when exposed to a predetermined stimulus, such as osmotic pressure, heat, UV light, etc.

1.6 Laponite

Laponite is a synthetic nanosilicate clay with a variety of applications in pharmaceutics and cosmetics, serving as a rheology-modifier. Laponite is available in a variety of forms, with Laponite XLG being the most commonly studied for biomedical applications. It has the empirical formula $Na_{0.7}^{+}[(Si_8Mg_{5.5}Li_{0.3})O_{20}(OH)_4]^{-0.7}$ and it consists of octahedral layers of magnesium oxide "sandwiched" between two parallel tetrahedral sheets of silica (Figure 5). The interlayer sodium cations are balancing the structure when it is in the form of a powder, but when dispersed in water, the sodium ions are released, which results in nanodiscs with average diameter of 20 nm and thickness of 1 nm. These nanodiscs present a negative charge on the platelet surface, whereas positive charges are distributed along the surface edges interacting with the interlayer cations. The laponite nanodiscs, at pH < 7.0, degrade into non-toxic components, hence it is considered a biodegradable and biocompatible material[29]. The last years, Laponite has been studied in 3D-printing for TE applications, exhibiting improved printing fidelity[30], and inducing osteogenesis while also offering a growth factor-free approach for bone tissue regeneration[31].

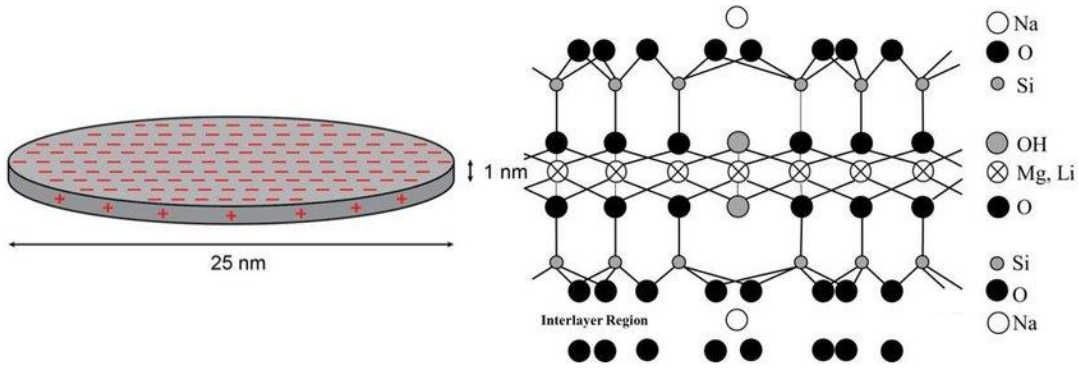

Figure 5: A Laponite nanodisc (left) and its single crystal (right)[44].

1.7 Characterization Techniques

1.7.1 Size Exclusion Chromatography (SEC)

Size exclusion chromatography (SEC) or gel permeation chromatography (GPC) is a chromatographic technique widely used for the characterization of polymeric materials. It is a convenient method that exploits the relative size or hydrodynamic volume of a macromolecule, in order to determine its average molecular weight and molecular weight distribution.

The standard SEC apparatus includes a pump, a detector (i.e. UV or IR or both) and a column. The column constitutes the stationary phase and it is filled with porous particles (i.e. silica, polystyrene etc.) of various pore diameters. The mobile phase is generally the same solvent used to dissolve the polymer and it is forwarded to the column through the pump. After injected in the flowing solvent system, the polymer elutes through the column, with the large molecules that cannot enter the pores of the packing, eluting first. The smaller molecules can penetrate or diffuse into or out of the pores resulting in later elusion times. Following their separation in the column, the chains pass through the detectors for final analysis. Since SEC is a relative technique,the columns must be calibrated with known molecular weight polymer standards.

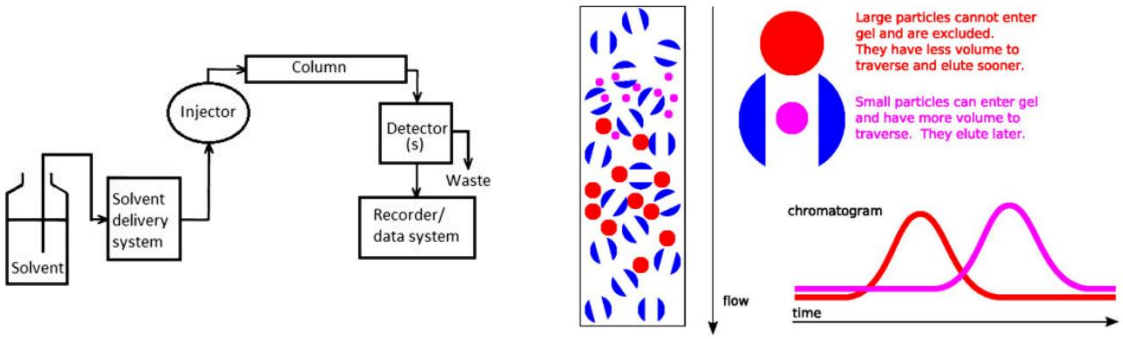

Figure 6: Schematic illustration of the SEC apparatus (left) and basic principles behind the SEC technique (right)[37].

1.7.2 Nuclear Magnetic Resonance (NMR) Spectroscopy

Nuclear magnetic resonance (NMR) spectroscopy is a non-destructive analytical technique used to determine the chemical structure of organic compounds and it is based on the fact that certain nuclei exhibit specific magnetic properties. When a sample is placed within the magnet of the NMR spectrometer, it is exposed to a strong external magnetic field, causing the alignment of half-integer spin nuclei (i.e. I=1/2, 3/2, etc). Subsequently, the sample is subjected to radiofrequency radiation which causes excitation of the lower energy level nuclei to a higher one. When the electromagnetic radiation stops, a signal at radiofrequencies characteristic of each isotope is generated and then converted by several detectors into a spectrum.

Various structural information can be extracted from an NMR spectrum. The precise resonant frequency of the energy transition is dependent on the different chemical environments and electron shielding of the nuclei. Thus, bonding to electronegative groups or hydrogen bonding, can change the electron density around the nucleus and shift the resonant frequency (chemical shift). Active neighbouring nuclei that are not chemically identical can cause spin coupling (spin-spin coupling), providing structural information too. In NMR spectra, this effect is shown through peak splitting and it is described by the relationship where n neighboring nuclei result in $n+1$ peaks. Also, the peak intensity can give information concerning the number of nuclei that created the peak, by measuring the area underneath using integration. Besides identification, structure and

environment, NMR spectroscopy can provide detailed information about the dynamics and reaction state of molecules. Last, the most common types of NMR are ^{1}H NMR and ^{13}C NMR, but it is applicable to any sample containing half-integer nuclei.

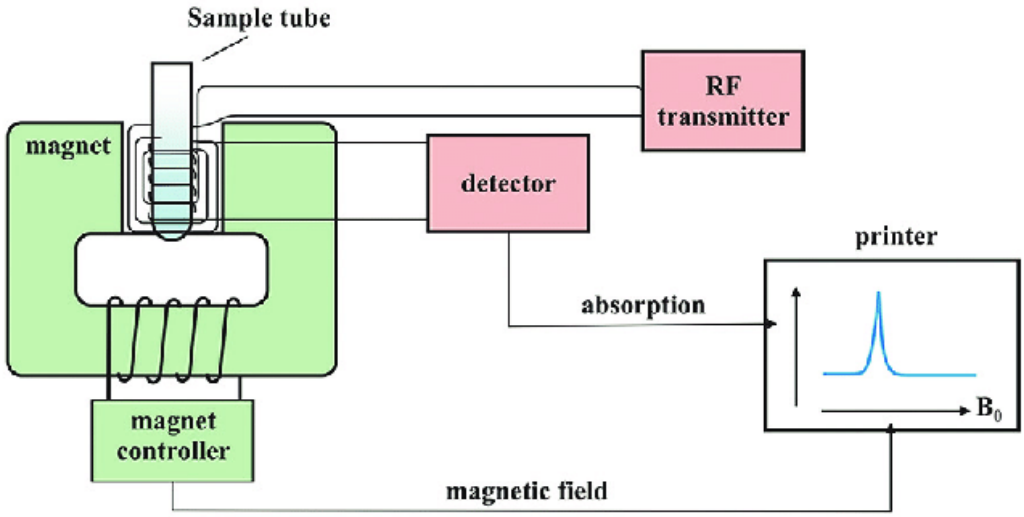

Figure 7: Schematic illustration of the NMR spectrometer instrumentation[38].

1.7.3 Attenuated Total Reflectance - Fourier Transform Infrared Spectroscopy (ATR-FTIR)

Attenuated total reflectance is a sampling technique that is used in combination with infrared spectroscopy as a nondestructive and reagent/solvent free physicochemical tool for the characterization of several samples, either solid or liquid. Additionally, the Fourier – transform process is required to convert the raw data into spectra.

The standard ATR-FTIR apparatus consists of an ATR crystal with a high refractive index that is in direct contact with the sample. When an infrared beam is directed onto the crystal, at a certain angle, it is internally reflected creating an evanescent wave that extends beyond the surface of the crystal, by a few microns (0.5 – 5 μ), into the sample held in contact with the crystal. Subsequently, the parts of the sample that absorb the beam's energy, cause the alteration or attenuation of the wave. The attenuated wave is passed to the detector in the IR spectrometer and is converted into a

spectrum. As with all FTIR measurements, the background collection of the clean crystal precedes the sample's measurement. ATR – FTIR spectroscopy, is applicable to many chemical or biological systems, as it provides fast sampling, improved sample-to-sample reproducibility and minimal spectral variation for different users[32].

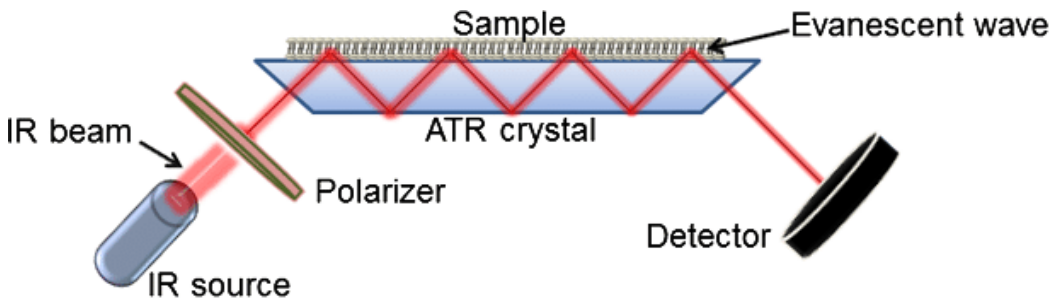

Figure 8: Simplified depiction of the ATR – FTIR operation mode[32].

1.7.4 Thermogravimetric Analysis (TGA)

Thermogravimetric analysis (TGA) is a technique that continuously measures the mass of a material as a function of temperature or time, while the sample is subjected to a predetermined temperature program in a controlled environment. Thus, it can provide information about physicochemical phenomena, such as vaporization, sublimation, adsorption, oxidation, thermal decomposition etc, that can occur while a material is undergoing thermal changes.

The sample is loaded on a pan positioned on a holder, which is connected with a microbalance. Next the material is heated by an electric furnace that can reach up to 2000 ℃, depending on the type of the material and pan (alumina, platinum, aluminum). The thermal processing can be performed under ambient air, vacuum, inert gas, etc. In general, it can be used for the study of polymeric materials, including thermoplastics, elastomers and composites, whereas it can be combined with other methods like differential scanning calorimetry, to identify unknown samples.

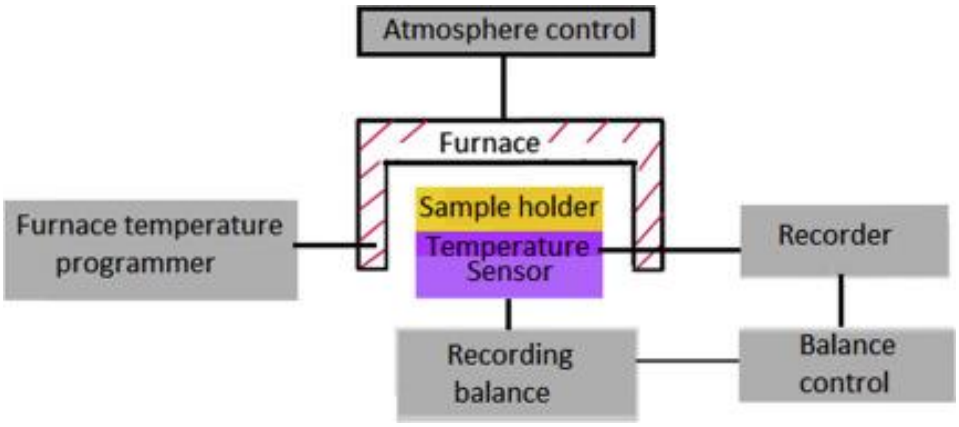

Figure 9: Graphic representation of a TGA set-up[39].

1.7.5 Differential Scanning Calorimetry (DSC)

Differential scanning calorimetry (DSC) is a technique used for the thermal analysis of various materials like polymers, biomolecules, nanomaterials, drug compounds, etc. DSC tracks the heat capacity (Cp) of a sample by measuring the changes in the heat flow during consecutive heating and cooling cycles. This allows the detection of several physical transformations, such as phase transitions, melting points, crystallization and glass transition changes.

The most common type of DSC is the heat-flux, in which a sample of a known mass, enclosed in a pan, and an empty reference pan are placed on a thermoelectric disk surrounded by a furnace. When the furnace is heated, both pans are heated through the thermoelectric holder and the heat flow is calculated by the difference in temperature (ΔT) between the sample and the reference. This difference would be the amount of excess heat absorbed or released by the sample during an endothermic or exothermic process, respectively[33]. Both endothermic (melting) and exothermic processes (crystallization), are shown as peaks, in a DSC curve of crystalline or semicrystalline materials. On the other hand, the glass transition of amorphous or semicrystalline materials, is shown as a step on the base line of the curve. In conclusion, DSC can be used as a thermo-analytical tool in chemical science, pharmaceuticals and food industry, as well as in protein studies.

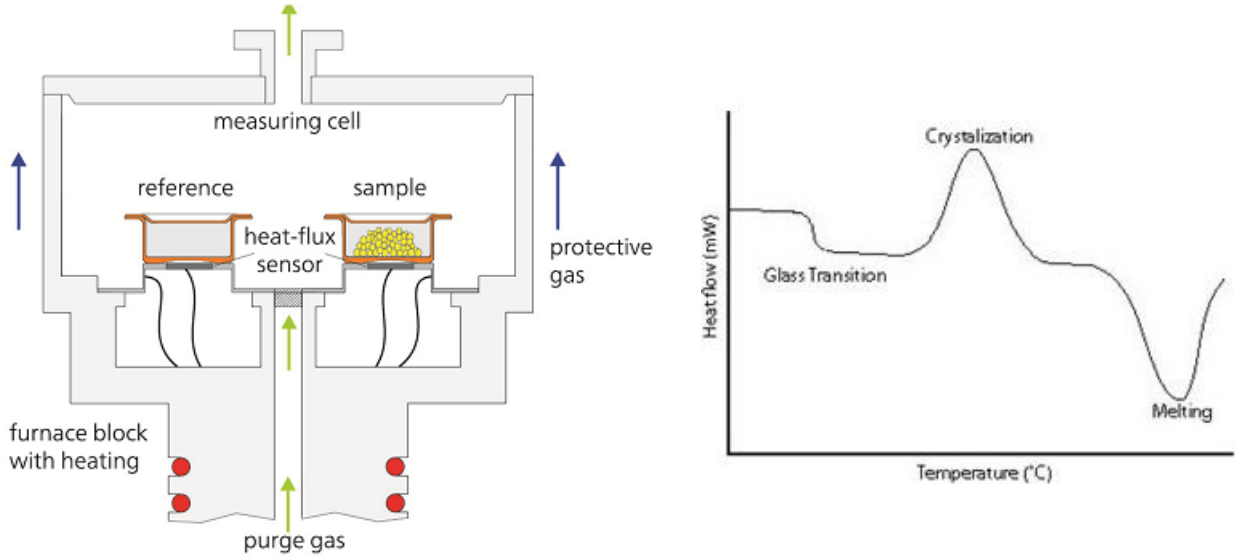

Figure 10: Image of the basic apparatus of a heat-flux DSC (left) and typical features of a DSC curve (right)[40].

1.7.6 Ultraviolet/Visible (UV-Vis) Spectroscopy

UV-Vis spectroscopy is used to determine the absorbance spectra of a substance in solution or in the solid state. The absorption of the light energy or electromagnetic radiation, which excites electrons from the ground state to the first singlet excited state of the chemical or substance, is what is being measured spectroscopically. The UV-Vis region of energy for the electromagnetic spectrum covers the range of 1.5 - 6.2 eV, which relates to the wavelength range of 800 - 200 nm. The principle behind the absorbance spectroscopy is the Beer-Lambert law:

$$A = \varepsilon \cdot b \cdot c$$

Where, A is the absorbance, ε is the molar absorptivity of the compound or molecule in solution ($M^{-1}cm^{-1}$), b is the path length of the cuvette or sample holder (usually 1 cm), and c is the concentration of the solution (M).

A typical UV-Vis spectrometer has a light source (deuterium or tungsten lamp), a sample holder and a detector, whereas some can also have filters for selecting one wavelength at the time. A reference cell with the solvent to calibrate the instrument is always required.

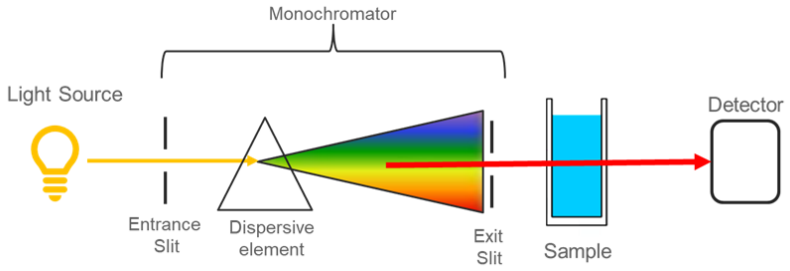

Figure 11: Schematic representation of UV-Vis spectroscopy[42].

1.7.7 Static Water Contact Angle (static WCA) measurements

Water contact angle (WCA) measurements is a means to quantify the wettability of a solid surface. Contact angle, θ, is defined geometrically as the angle formed by a liquid at the three-phase boundary where a liquid, gas, and solid intersect. At a given temperature and pressure, a given system of solid, liquid, and vapor has a unique equilibrium contact angle. The sessile drop or static contact angle is the most simple contact angle technique. This is when the liquid drop is static on the surface. However, depending on the characteristics such as the chemical homogeneity, topography, and roughness, there is a variety of contact angles on surfaces. Dynamic advancing and receding contact angles can be measured to capture the whole range of angles for a particular surface. The discrepancy between the advancing and retreating angles is defined as contact angle hysteresis. Hysteresis is caused by the chemical and topographical heterogeneity of a surface, solution impurities absorbing on the surface, swelling, rearrangement, or change of the surface by the solvent.

Modern optical tensiometers, analyze the liquid's drop shape by taking images of the drop with a digital camera. The drop is then fit with the Young-Laplace equation with the tangent line drawn from the baseline of the drop to the edge. The droplet can be dispensed either manually, or

automatically, but in both cases, a given volume of water is deposited on the surface of interest by a needle tip or pipette that is gently brought into contact with the surface of interest.

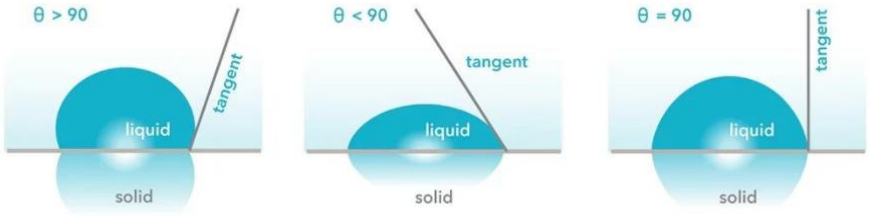

Figure 12: Different contact angles on a surface[43].

1.7.8 PrestoBlue™ Cell Viability Assay

The PrestoBlue™ cell viability assay is a commonly used technique for determining the cytotoxicity of the compounds under examination. It is a colorimetric approach based on resazurin that allows for the indirect measurement of the number of live cells, by calculating the level of reduction of resazurin in the environment of the cells. Resazurin has a deep blue color when oxidized, but it becomes purple when reduced. The intensity of the purple color is proportional to the reduction potential of the live cells, allowing cell viability to be quantified using a spectrophotometer.

1.7.9 Scanning Electron Microscopy (SEM)

Scanning electron microscopy (SEM) is one of the most common methods used to image the microstructure of materials. SEM is an electron microscopy method that uses a focused intense electron beam to examine the surface of a material. An electron gun fires this beam, which then accelerates down the column of the scanning electron microscope. During this process, the electron beam is focused by passing through successive lenses and apertures. This occurs under high vacuum conditions, which prevents any molecules or atoms from interacting with the electron beam. The electron beam sweeps across the sample in a dense grid, scanning the surface area in lines from side to side and top to bottom. The electrons interact with the atoms on the surface of

the sample, which create signals in the form of secondary electrons, backscattered electrons and rays that are characteristic of the sample and are analyzed by the detectors creating high resolution images.

1.8 Current Study

Driven by the increasing interest on polyesters, as promising materials for tissue engineering applications, and the lack of research with regards to polyesters with pH-responsive behavior, we aimed in this work in the development of functional, pH-sensitive aliphatic polyesters. The newly acquired materials were synthesized in a two-step procedure. First, the precursor alkene-bearing polyester was synthesized via a facile polycondensation polymerization between two commercially available compounds, a diol and a diacid chloride, namely trimethylolpropane allyl ether and adipoyl chloride, respectively. The presence of alkene side groups offers great advantages, since they can be easily modified via appropriate post-polymerization chemistries. Thus, in a post-synthesis approach, using a photosensitive, thiol-ene click reaction, two distinct mercaptocarboxylic acids with different chain lengths, were coupled onto the precursor polyester. 3-Mercaptopropionic and thioglycolic acid were used to synthesize polyesters bearing different fractions of alkene/carboxylic acid side groups, by varying the irradiation time during the reaction. At the same time, the pH–responsive behavior was introduced to the polyesters by the carboxylic acid groups. The influence of the side chain length and the degree of carboxylic acid-functionalization on the pK_α and the water solubility of the polymer, were studied. To evaluate the cytocompatibility of the functional polyesters, thin films were prepared by spin coating on pre-silanized glass substrates bearing polymerizable methacrylate groups. The films were covalently attached onto the substrates by a photo-induced free-radical coupling of the pendant alkene moieties. The polymer films' potential as culture substrates was investigated by evaluating the cell viability, proliferation, adhesion, and morphology of L929 fibroblasts cultured on them. The polyester showing the best cytocompatibility, PE-Glyc80, was selected for the development of a pH-sensitive 3D-printable biomaterial for tissue engineering applications. The printing fidelity of the material improved when it was pre-crosslinked with PEGDMA 750, resulting in a soft, easily extruded hydrogel that was UV-treated to secure the 3D-printed structure. Finally, laponite, a nanoclay widely used in tissue engineering applications, was blended with the polyester, following

the same conditions for the 3D-printing, to boost the bioactivity of the scaffolds. Both fabricated 3D scaffolds were evaluated in terms of degradability in physiological pH and the influence of the pH on the swelling properties and the porosity of the structures.

Chapter 2

2. Experimental Part

2.1 Materials

Trimethylolpropane allyl ether (98%), adipoyl chloride (98%), pyridine (99.5%), 3-mercaptopropionic acid (≥99%), thioglycolic acid (98%), 3-(trimethoxysilyl) propyl methacrylate (98%), 2,2-dimethoxy-2-phenyl-acetophenone (99%), chloroform (≥99.8%), methanol (≥99.8%), dimethylformamide (≥99.8%), and Hellmanex III were purchased from Sigma-Aldrich (Steinheim, Germany). Ethanol (≥99.8%) was obtained from Honeywell (Seetze, Germany) and toluene (≥99.8%) from Fisher Scientific (Loughborough, UK). Dichloromethane (analytical grade), n-hexane (96%), and diethyl ether (99.8%) were purchased from Scharlau (Sentmenat, Spain). Dichloromethane was dried over calcium hydride and distilled under a nitrogen atmosphere prior to use. All the other solvents and chemicals were used without further purification. Trypsin/EDTA (0.25%), phosphate buffer saline, Amphotericin-B (fungizone), penicillin/streptomycin (P/S), were all purchased from Gibco ThermoFisher Scientific (Waltham, MA, USA), Roswell Park Memorial Institute 1640 medium (RPMI) with stable glutamine and fetal bovine serum from PAN-Biotech (Aidenbach, Germany) and PrestoBlue™ reagent for cell viability from Invitrogen Life Technologies (Carlsbad, CA, USA). The L929 fibroblastic cell line was purchased from the German collection of microorganisms and cell cultures (DSMZ GmbH, Braunschweig, Germany).

2.2 Characterization Methods

2.2.1 SEC

The molecular weights and the molecular weight distributions of the polyesters were determined by SEC utilizing a Waters-515 isocratic pump equipped with two columns, Mixed-D and Mixed-E (Polymer Labs), a Waters 2745 Dual Absorbance detector and a Waters 410 refractive index (RI) detector. Tetrahydrofuran (THF) with 2 v/v% triethylamine (TEA) was used as the eluent at a flow 1 ml/min. The molecular weights of the polymers were determined by the universal calibration method using eight narrow molecular weight PMMA standards ranging from 875 to 138,600 gr/mol. In a typical measurement, 20 mg of the polymer were dissolved in 1 ml THF

(HPLC) with 1 v/v% toluene, filtered through a PTFE filter with pore size 0.45 μm and was injected to the system (20μL).

2.2.2 ^{1}H-NMR

The synthesized functional polyesters were characterized by ^{1}H NMR spectroscopy using Avance Bruker AMX-500 and a DPX-300 spectrometer (Bruker, Rheinstetten, Germany). Spectra were recorded in $CDCl_3$ or acetone-d6 as the deuterated solvents at 25 ℃.

2.2.3 ATR-FTIR

The ATR-FTIR spectra were recorded on a Nicolet 6700 spectrometer (Thermo Fisher Scientific, Waltham, MA, USA). For each spectrum, 128 scans were collected in the 500–4000 cm^{-1} range.

2.2.4 Potentiometric Titrations

The aqueous solution behavior of the synthesized polyesters bearing carboxylic acid side groups was investigated as a function of the solution pH by potentiometric titration measurements. In a typical experiment, first, the polymer was dissolved in water at 1 wt% and the solution pH was adjusted to pH~12 using 0.1 M NaOH. After stirring for 30 min at RT, the polymer solution was titrated using 20–100 μL aliquots of 0.01 M HCl and the decrease of the solution pH was monitored as a function of the amount of acid added. One minute equilibration time was allowed between each addition of the titrant. The pH was measured with a WTW inoLab pH7110 (Xylem Analytics Germany Sales GmbH & Co. KG, Weilheim, Germany) pH meter and titration curves in the pH range from 12 down to 3 were obtained.

2.2.5 Turbidimetry

The pH-dependent solubility of the carboxylic acid functionalized polyesters was studied by optical transmission measurements at λ = 650 nm using a Perkin Elmer Lambda 25 UV/Vis

Spectrophotometer (Perkin Elmer, Llantrisant, UK). For this, a 1 wt.% aqueous polymer solution at pH 12 was prepared and the pH of the solution was gradually decreased by the addition of 20–100 μL aliquots of 0.1 M HCl. The transmittance of the solution was measured as a function of the solution pH at room temperature.

2.2.6 TGA

TGA was performed using a Perkin Elmer Pyris Diamond TG/DTA instrument (Perkin Elmer, Llantrisant, UK). In a typical measurement, 15 mg of the sample were placed in an aluminum holder and were heated under a constant N_2 flow, from room temperature up to 550 ℃, at a heating rate of 10 ℃/min.

2.2.7 DSC

DSC was performed on a Waters TA DSC250 Discovery Series instrument (Waters TA, New Castle, UK). In every measurement, a small amount of the sample (<5 mg) is loaded on the DSC holder, and the heat flow was monitored as a function of temperature ranging from -100 to 200 ℃ with a heating rate of 10 ℃/min for 2 subsequent cycles of heating and cooling. All data presented are from the second cycle.

2.2.8 Profilometry

The thickness of the films was measured using a Veeco Dektak 150 Optical Profilometer (Plainview, NY, USA).

2.2.9 Static WCA measurements

The wettability of the polymer films was assessed by static WCA measurements using a contact angle goniometer (OCA- 40, DataPhysics Instruments GmbH, Filderstadt, Germany) and the sessile drop method. A 5 μL droplet of nanopure water was used and the contact angles were

calculated from the digital images of the water droplets deposited on the surfaces, recorded by a camera, using the appropriate software. Each measurement was carried out five times (n = 5).

2.2.10 Optical Microscopy

The cell seeded polyester films were observed using an inverted optical microscope (Axiovert 200, Carl Zeiss, Berlin, Germany) and the photographs were taken by employing a ProgRes CF scan camera and its compatible software ProgRes Capture Pro (Jenoptik Optical Systems GmbH, Berlin, Germany). In order to evaluate the cell adhesion and morphology, optical microscopy images were obtained for each sample at day 4, as the morphological features of cells can be well recognized at this particular experimental time point due to their moderate number, and were compared to the tissue-culture-treated polystyrene (TCPS) control surface.

2.2.11 Cell Viability and Proliferation Assay

The PrestoBlue™ assay was conducted after 2, 4, and 7 days in culture. Following the removal of the culture medium, the cells were incubated for 1 h at 37 ℃ in a mixture of PrestoBlue™ and fresh medium at a ratio of 1:10 v/v. Next, 100 μL of the mixed solution from every sample were transferred into a 96-well plate and the absorbance was measured at 570/600 nm in a spectrophotometer (Synergy HTX Multi-Mode Microplate Reader, BioTek, Bad Friedrichshall, Germany). Following the measurements, the culture medium was replaced in each well. Three independent experiments each in triplicates (n = 9) were performed and analyzed to evaluate the cell viability.

2.2.12 Statistical Analysis of the Cell Viability

The GraphPad Prism software version 8.0 (GraphPad Software, San Diego, CA, USA) was used to perform the statistical analysis of the cell viability experiments. Specifically, the statistical analysis was conducted using the ANOVA t-test method in order to determine the statistical significance of cell viability between the cells seeded on the polyester films and the TCPS control.

The analysis was performed for each experimental time point (day 2, 4, and 7). A p-value of <0.05 is considered statistically significant and was designated with one asterisk, $p < 0.01$ is depicted with two asterisks, and $p < 0.001$ with three asterisks.

2.3 Synthesis of poly(TPAE-*alt*-AD)

The functional polyester with pendant alkene groups was synthesized by a condensation copolymerization of a diol and a diacyl chloride, as described by Yan and coworkers[34]. In a typical procedure, adipoyl chloride (ADC) (8.43 mL, 57.97 mmol) was added dropwise in a solution of trimethylolpropane allyl ether (TPAE) (10 mL, 57.97 mmol) in freshly distilled dichloromethane (DCM) (120 mL), containing dry pyridine (10.31 mL, 127.53 mmol) under a N_2 atmosphere, in an ice bath. The polymerization was allowed to proceed for 67 h at room temperature. Subsequently, the salt formed was removed by filtration and the filtrate was evaporated using a rotary evaporator to reduce the volume of the solution. The final product was collected by precipitation in cold methanol.

2.4 Synthesis of Functional Polyesters with Carboxylic Acid Side Groups

The polyester bearing alkene side groups, poly(TPAE-*alt*-AD), was modified using mercaptocarboxylic acids via a pho-induced thiol-ene reaction, to obtain the carboxylic acid functionalized polyesters. For this, poly(TPAE-*alt*-AD) (1.25 g, 4.40 mmol) and dimethylformamide (DMF) (5 mL) were introduced in a Schott–Duran round-bottom flask, while 2,2-dimethoxy-2-phenylacetophenone (DMPA) (0.2 eq., 225.6 mg, 0.880 mmol) was added as the free-radical photoinitiator. The mixture was stirred with 3-mercaptopropionic acid (1.5 eq., 575 μL, 6.60 mmol) or thioglycolic acid (1.5 eq., 458.8 μL, 6.60 mmol) for 15 min, under a N_2 atmosphere, at room temperature. Next, each solution was irradiated with UV light (λ= 365 nm). Three copolymers, with a degree of modification of the alkene side groups to carboxylic acid moieties of 50%, 80%, and 100%, were prepared by varying the irradiation time. Finally, the reaction mixture was dialyzed against methanol for 24 h to remove the unreacted

mercaptocarboxylic acid, the photoinitiator, and DMF. The purified product was collected by precipitation in a cold n-hexane/diethyl ether mixture (ratio 50:50).

2.5 Preparation of Polyester-Based Thin Films

Thin films of the functional polyesters were prepared on glass coverslips (100 μm thickness, 13 mm diameter). First, the glass substrates were sonicated in a Hellmanex aqueous solution for 30 min, followed by thorough rinsing with deionized water and drying under a N_2 gas stream. Subsequently, the coverslips were immersed in a 5 v/v% solution of 3-(trimethoxysilyl)propyl methacrylate (MAPTMS) in anhydrous toluene, under a N_2 atmosphere, at room temperature for 18 h. Next, the modified substrates were extensively washed with toluene and were finally dried with a N_2 gas stream. Separately in a vial, a 10 w/v% solution of the functional polyester in chloroform ($CHCl_3$) was prepared, and 1 wt.% of DMPA was added as the photoinitiator. The solution was filtered twice through a PTFE syringe filter (0.45 μm) and 100–200 μL of the filtered solution were spin coated, using an SPS spin coater (1600 rpm, 120 s, 1000 rpm/s), on the MAPTMS modified glass substrates. The films of the alkene functional polyesters were next crosslinked via their vinyl pendant moieties and were bound to the methacrylate double bonds of the substrate by irradiation with UV light (λ = 365 nm) for 90 min. Finally, the films were dried overnight under vacuum at 40 ℃ and were next rinsed multiple times with ethanol and deionized water before use.

2.6 Cell Culture of L929 and Seeding onto Polyester Thin Films

The biocompatibility assessment was conducted using L929 fibroblast cells of passage 13 and lower (cat. No. ACC-2, DSMZ GmbH, Braunschweig, Germany). The L929 cell line was chosen primarily due to the excellent adaptability that the fibroblasts present to different environments, making them ideal for cytocompatibility testing. Cells were cultured in a humidified incubator at 37 ℃ and 5% CO_2 in RPMI 1640 culture medium (w/s stable glutamine), enriched by the addition of 10% fetal bovine serum (FBS), 1% penicillin/streptomycin, and 1% amphotericin B. The cells were trypsinized using a 0.25% trypsin/EDTA solution when they reached their maximum level

of confluency. For each cell viability and adhesion experiment, 2×10^4 cells were seeded onto the modified polyester films spin coated on glass substrates in 24-well plates. The same number of cells was seeded onto TCPS wells used as a control surface. Prior to the cell seeding, the polyester films were sterilized by exposure to UV light for 15 min and washed once with the culture medium. Then, a 10 μL drop of the cell suspension was added into each well, which was then filled with 500 μL culture medium, and the plate was placed in a humidified cell culture incubator (ThermoFisher Scientific, Roskilde, Denmark). Medium change was carried out every two to three days.

2.7 Preparation of the Pre-Crosslinked Hydrogels

For the 3D printing procedure, the carboxylic acid-functionalized polyesters with > 85% degree of functionalization were used. The selected polyester was pre-crosslinked to become more robust and thus printable. For this, a 25 w/v% solution of PE-Glyc85 (0.5 g, 1.38 mmol) in a acetone/H_2O (90:10) mixture were introduced in a Scott-Duran round-bottom flask, while DMPA (0.2 eq., 70.9 mg, 0.277 mmol) was added as the free-radical photoinitiator. The mixture was stirred with poly(ethylene glycol) dimethacrylate with average M_n 750 g/mol (0.15 eq., 141.6 μL, 0.207 mmol), as the crosslinker, for 20 min under a N_2 atmosphere, at room temperature. The laponite hydrogels were prepared by addition of 3 % w/v (60 mg) laponite in the polymer mixture. Next, the solution was irradiated with UV light (λ = 365 nm) for 4 min, until gelation. The hydrogel was collected with a spatula and placed inside a syringe tube for use in 3D printing.

2.8 3D Printing

The pre-crosslinked polyester and polyester/laponite hydrogels were loaded in a 3 ml syringe which was connected with a 3 ml cartridge via a female/female luer lock adapter (Cellink, Sweden). The hydrogel cartridge was printed with a 22G high-precision blunt needle (Cellink, Sweden) using a Inkredible+ bioprinter (Cellink, Sweden). The design of the multi-layered construct was made using the software provided by www.tinkercad.com. The 3D object was saved in a stl. file which was sliced using Slic3r and a Gcode file was produced, that can be read by the

printer. The construct has some intersected lines which hindered the multi-layered result, as shown in Figure 13. Next, the 10-layer constructs were printed on petri dishes at room temperature at a speed of 1200 mm/min, pressure 280 kPa and a layer height of 0.25 mm. Finally, the scaffolds were UV-cured (λ = 365 nm) for 20 min to further secure the integrity of the structures.

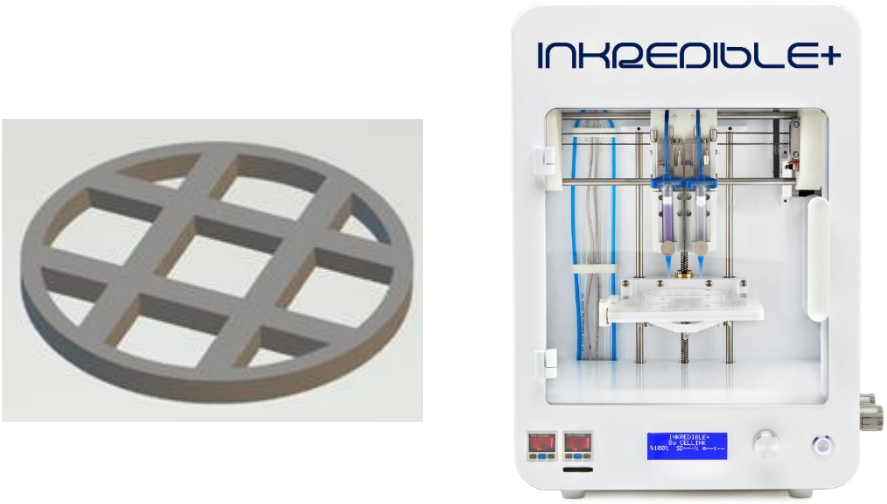

Figure 13: The 3D-object as designed with the software (left) and the Inkredible+ bioprinter (right).

2.9 Degradation

For the degradation of the pH-responsive 3D-printed hydrogels, 25-40 mg of the hydrogels were thoroughly rinsed in acetone and then dried overnight at 60 ℃. Next, the dried hydrogels were immersed in vials containing 2 ml PBS buffer which with adjusted at pH 7.4 at 37 ℃. At predetermined time intervals, the mass of the swollen hydrogel was measured, and the degradation (%) of the hydrogel was calculated using the following equation:

$$Degradation\ Degree\ \% = \frac{Mo - Mt}{Mo} \cdot 100\%$$

Where, Mo is the initial mass of the dried hydrogel and Mt is the mass of the hydrogel measured at each time point, t.

2.10 Swelling behavior of the 3D constructs

In order to investigate the degree of swelling of the pH responsive 3D printed hydrogels, 25-40 mg of the hydrogels were soaked in acetone for 3 h to remove any unreacted molecules and were then dried overnight at 60 ℃. Next, the dried hydrogel was immersed in vials containing 2 ml of a buffer of different pH value (acetate buffer: 3.0, PBS: 6.0, 7.4, Sodium carbonate/bicarbonate: 9.2). At predetermined time intervals, the hydrogels were placed on tissue paper to effectively remove the excess buffer and then the mass of the swollen hydrogel was measured. The % degree of swelling of the hydrogel was calculated using the following equation:

$$Degree\ of\ Swelling\ \% = \frac{Ws - Wd}{Wd} \cdot 100\%$$

Where, Ws is the weight of the swollen hydrogel and Wd the weight of the dried hydrogel.

2.11 SEM

For the SEM imaging of the 3D scaffolds, a 20 nm Au film was deposited by sputtering on the freeze-dried samples to prevent charging of the surface during the measurement.

Chapter 3

3. Results and Discussion

3.1 Synthesis and Structural Characterization of Alkene Functionalized Polyesters

The polyester poly(TPAE-*alt*-AD) containing pendant alkene groups was prepared by a simple polycondensation reaction between TPAE, which is an alkene functionalized diol, and a diacyl chloride with six carbon atoms, namely adipoyl chloride (ADC). Following a similar synthetic approach, described previously by Yan et al.[34], the polymerization was carried out at room temperature with no metal catalyst present (Sch. 1). Pyridine is used as the promoter of the polymerization, as it eliminates the byproduct of the reaction (HCl), by forming pyridine hydrochloride. The ideal reaction time was estimated at around 67 h, when the number average molar mass and the molecular weight distribution of the polyester calculated by SEC analysis were around 28,000 g/mol and 1.3 respectively, whereas the reaction yield was 60 %. When the reaction time was greater than 67 h, the polyester molecular weight and the reaction yield decreased, as displayed by SEC analysis in Figure 14, which is attributed to the hydrolysis of the ester bonds (Table 2). To obtain the final product, the polyester was precipitated in methanol, which removes any chloride residues and lower MW oligomers, decreasing the final polydispersity, as shown by SEC in Figure 15 (Table 3). The relatively broad polydispersity of the polymer is overall expected for a polycondensation reaction.

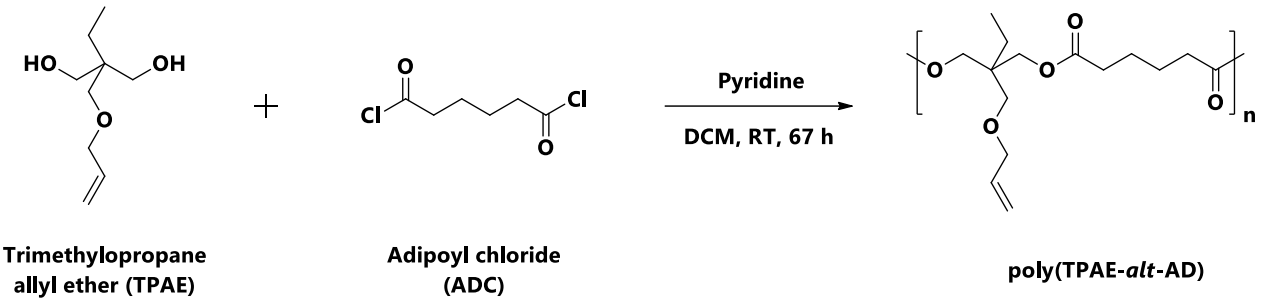

Scheme 1: Synthetic procedure followed for the preparation of the poly(TPAE-alt-AD) polyester.

The successful synthesis of poly(TPAE-*alt*-AD) was also confirmed by ^{1}H NMR analysis. Two characteristic peaks at 1.63 ppm (He) and 2.32 ppm (Hd), attributed to the adipoyl monomer repeat units, and two peaks at 5.82 ppm (Hh) and 5.0–5.3 ppm (Hi), assigned to the vinyl group present in the TPAE monomer repeat units, were observed, verifying the successful synthesis of the poly(TPAE-*alt*-AD) polyester (Figure 16).

Table 2: Molecular size characteristics of the synthesized polyesters at different reaction times.

Reaction time (h)	**Mn**	**Mw**	**Đ**	**% yield**
67	27957	37247	1.41	60 %
93	16121	21734	1.35	46 %

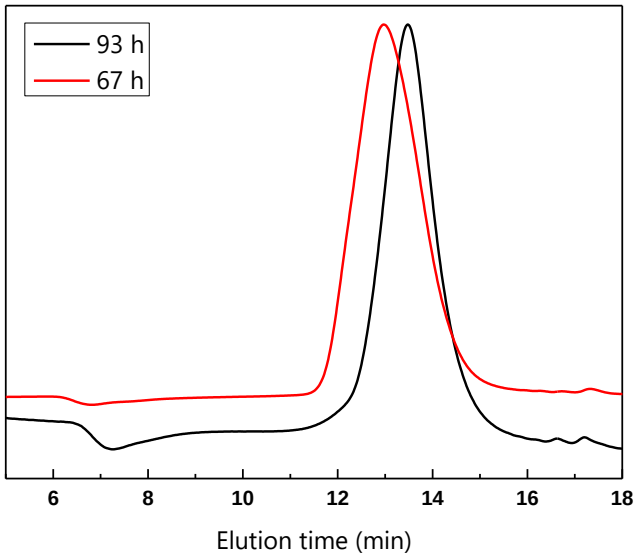

Figure 14: SEC curves of poly(TPAE-*alt*-AD) after 67 and 93 h reaction time.

Table 3: Molecular size characteristics of the synthesized polyesters before and after precipitation in methanol.

Precipitation in methanol	Mn	Mw	Đ
No	16471	36953	1.98
Yes	27957	37247	1.33

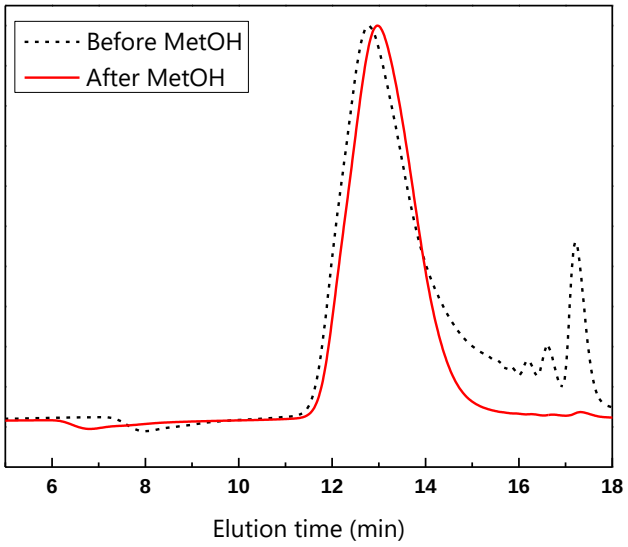

Figure 15: SEC curves of poly(TPAE-alt-AD) before and after precipitation in methanol.

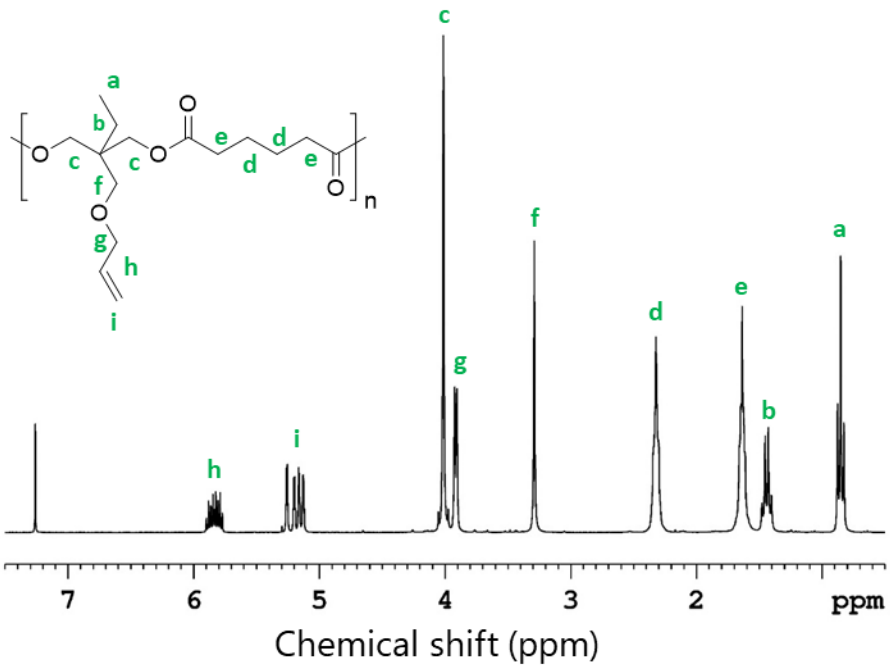

Figure 16: ^{1}H NMR spectrum of the poly(TPAE-alt-AD) polyester in which the peaks labeled (a-i) correspond to the protons of the polyester shown above.

3.2 Synthesis and Structural Characterization of Carboxylic Acid-Functionalized Polyesters

The alkene-containing polyester was functionalized with carboxylic acid pendant groups via a photo-induced thiol-ene click reaction, resulting in pH-responsive polyesters. For this purpose, thioglycolic acid (Glyc) or 3-mercaptopropionic acid (Prop), containing two and three carbon atoms, respectively, were reacted with poly(TPAE-*alt*-AD), to produce two distinct polyesters with carboxylic acid side groups found along the polymer backbone (Sch. 2). It is expected that the different alkyl chain length of the side groups, as well as the carboxylic acid functionalization degree, will influence both the physicochemical and biological properties of the pH-responsive polyesters.

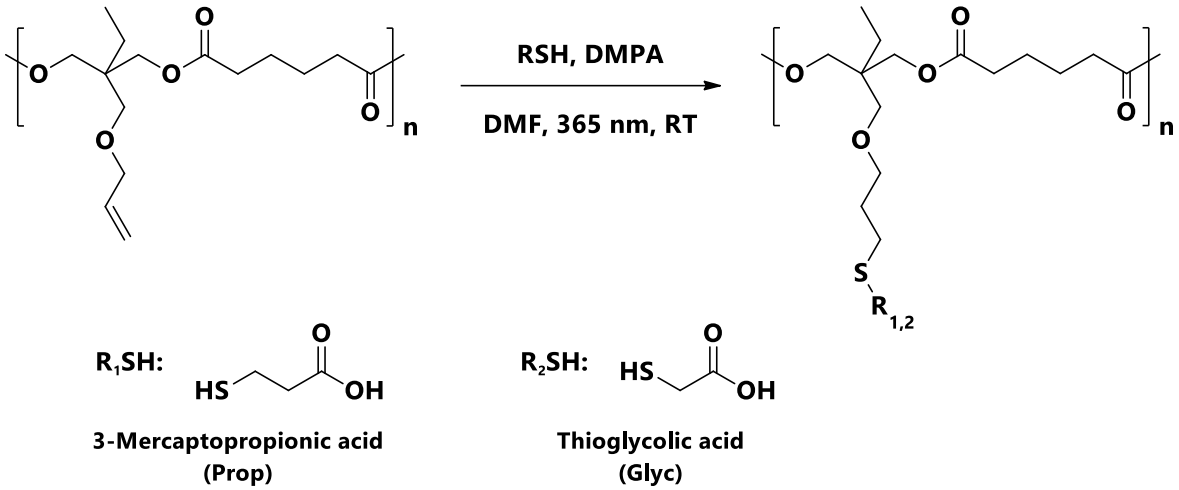

Scheme 2: Synthetic procedure followed for the preparation of the pH-responsive polyesters containing carboxylic acid side groups of different alkyl chain lengths.

The photo-induced thiol-ene click reactions were performed at room temperature using a UV-lamp emitting at 365 nm, with DMPA acting as the photoinitiator. To obtain partially carboxylic acid-modified polyesters, the molar ratio of the mercaptocarboxylic acids with respect to the alkene-bearing polyester and the duration of irradiation were studied. As expected, a molar excess of the mercaptocarboxylic acid leads rapidly to fully functionalized polyesters, whereas when the molar ratio is equal to one, the polyester is crosslinked forming non-soluble gels, indicating that the reaction between the remaining alkene groups of the polyester is favored, as opposed to the thiol-ene. Consequently, a lower excess of mercaptocarboxylic acid with respect to the pendant alkene groups of the polyester was used, offering perfect temporal control. In this way, polyesters with 50%, 80%, and 100% carboxylic acid side groups were obtained by varying the irradiation time from 60 s, 180 s, and 5 min for 3-mercaptopropionic acid and 40 s, 60 s, and 4 min for thioglycolic acid, at a constant mercaptocarboxylic acid/alkene mole ratio of 1.5. The names assigned to the synthesized polyesters were PE-GlycXX and PE-PropXX, where PE stands for the polyester main chain, Glyc and Prop represent the glycolic acid and propionic acid side groups, and XX represents the degree of modification of the alkene groups to the carboxylic acid functionalities. Thus, the propionic acid functionalized polyesters are represented as PE-Prop50, PE-Prop80, and PE-

Prop100, whereas glycolic acid functionalized polyesters are represented as PE-Glyc50, PE-Glyc80, and PE-Glyc100.

Table 4: Effect of reagent mole ratio on the degree of functionalization to the carboxylic acid functional polyesters.

Molar ratio (carboxylic acid:alkene groups)	**Results**
10.0 eq.	Fully functionalized
5.0 eq.	Fully functionalized
2.0 eq.	Fully functionalized
1.0 eq.	Gel formation
1.5 eq.	Temporal control

^{1}H NMR spectroscopy was used to investigate the successful polymer modification to bear carboxylic acid pendant groups, and to quantify the degree of modification of the polyester (Figures 17 and 18). Concerning the PE-Prop polyester, three new peaks appear at 1.82 ppm (Hh'), 2.61 ppm (Hi', Hj), and 2.75 ppm (Hk), which are assigned to the newly formed thioether groups and the attached propionyl group, verifying the successful polymer modification. The degree of modification was determined by comparing the peak integrals of the polymer backbone methylene protons (Ha), at 0.89 ppm, to the remaining vinyl protons (Hh and Hi), at 5.86 ppm and 5.0–5.3 ppm, respectively. The ratio of the peak integrals confirmed the degree of functionalization of the vinyl groups to the carboxylic acid moieties in the three samples being 49%, 83%, and 100%. In a similar way, the ^{1}H NMR spectra of the PE-Glyc polymers showed three new peaks at 1.85 ppm (Hh'), 2.72 ppm (Hi'), and 3.25 ppm (Hj), assigned to the newly synthesized thioether groups and the coupled glycolic group and confirmed the effective modification of the polyester. The degree of functionalization of the polyester with carboxylic acid groups was calculated as previously, by ratioing the integrals of the peaks at 5.87 ppm (Hh) and 5.0–5.3 ppm (Hi) to the peak at 0.89 ppm (Ha), and was found to be 46%, 83%, and 100% for the three polymers.

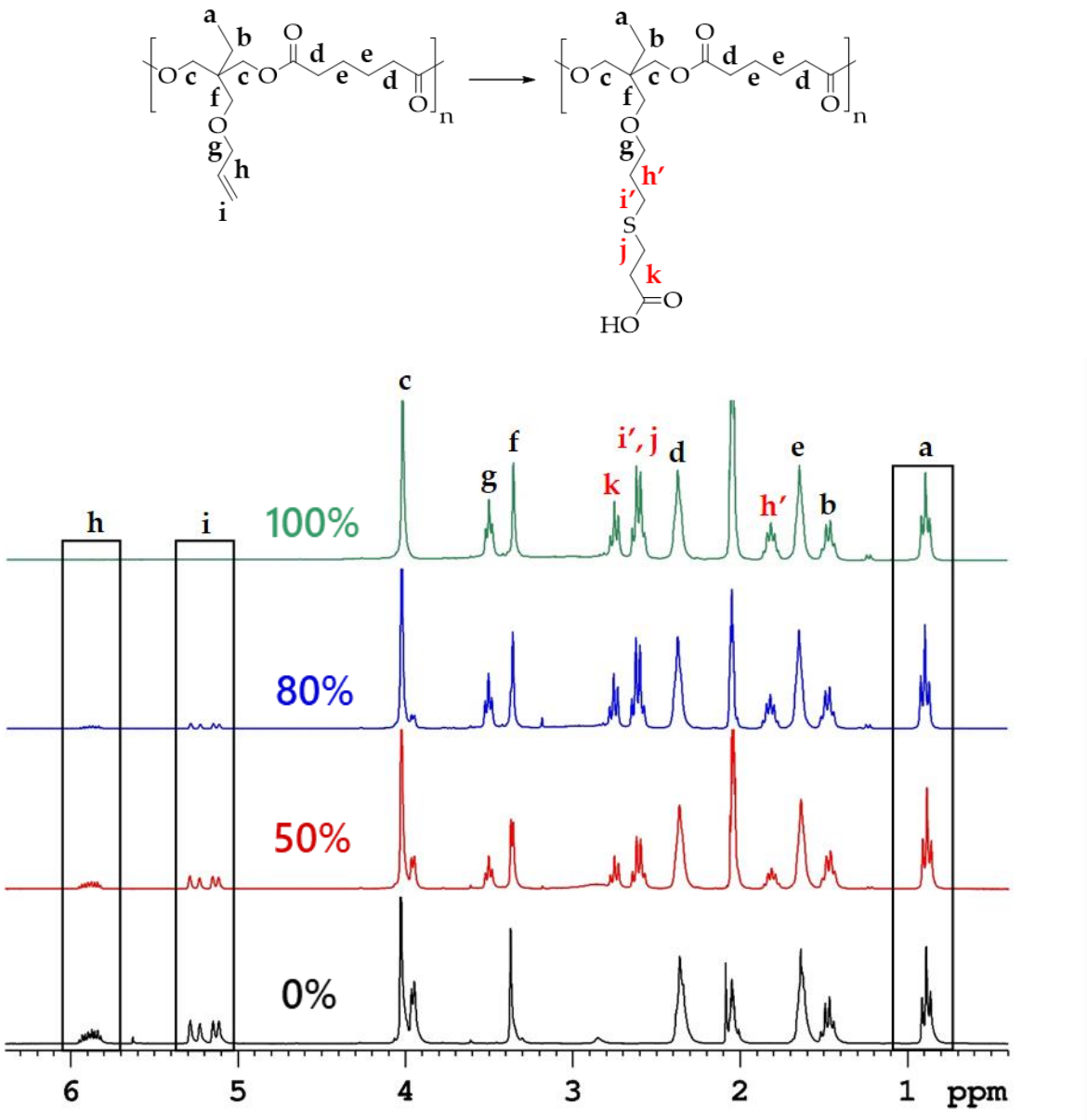

Figure 17: [1]H NMR spectra of poly(TPAE-alt-AD) (black line), PE-Prop50 (red line), PE-Prop80 (blue line), and PE-Prop100 (green line) in d6-acetone, in which the peaks labeled (a–k) correspond to the protons of the repeat units of the polyester shown on the top.

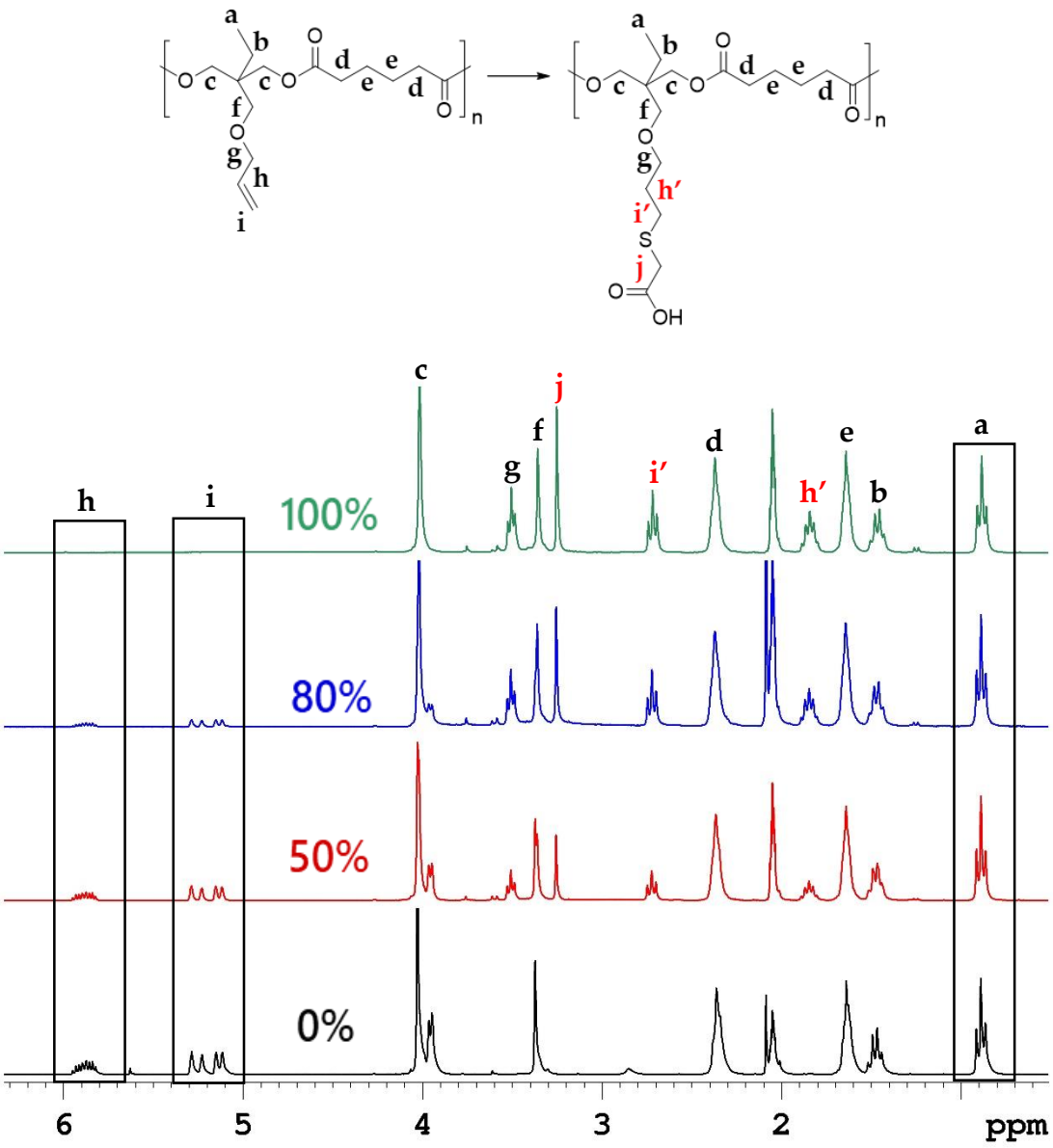

Figure 18: ^{1}H NMR spectra of poly(TPAE-alt-AD) (black line), PE-Glyc50 (red line), PE-Glyc80 (blue line), and PE-Glyc100 (green line), in d6-acetone, in which the peaks labeled (a–k) correspond to the protons of the repeat units of the polyester shown on the top.

ATR-FTIR spectroscopy was also used to characterize the functional polyesters (Figure 19). The ATR-FTIR spectra of the carboxylic acid-functionalized polyesters, show a new peak at about 1705 cm^{-1} attributed to the stretching vibration of the C=O bond of the carboxylic acid moieties and a decrease of the stretching vibrations assigned to the C=C bond of the vinyl side groups at about 1646, 990 and 925 cm^{-1}, confirming the effective derivatization of the polymer. As the degree of modification of the vinyl groups increases, the intensity of the peak attributed to the carbonyl bond of the carboxylic acid groups gradually increases, while the intensity of the peaks due to the carbon–carbon double bond monotonically decreases, confirming the ^{1}H NMR results discussed above.

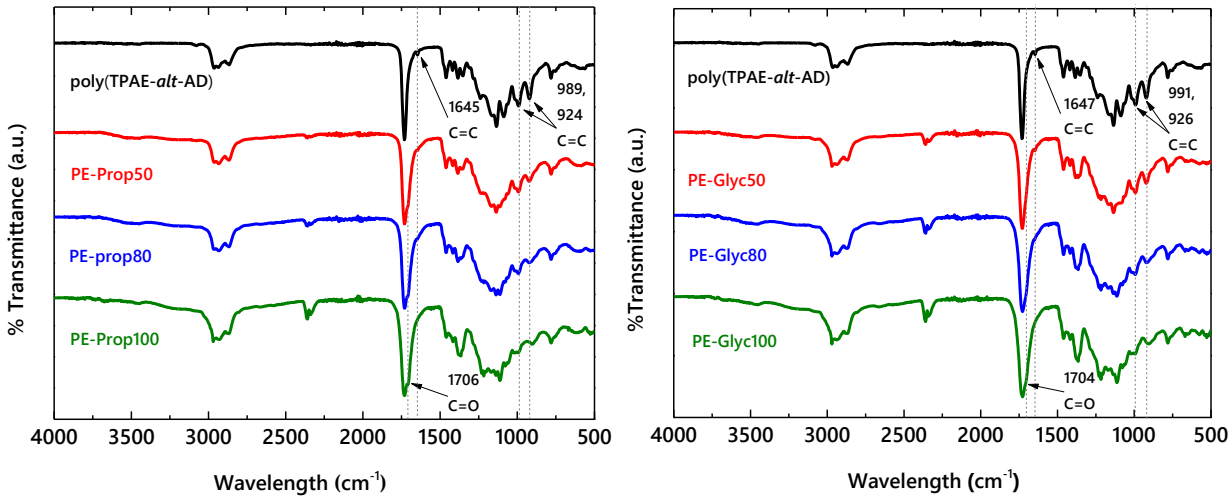

Figure 19: ATR-FTIR spectra of the PE-PropXX (left) and PE-GlycXX (right) polyesters.

3.3 Thermal Characterization of the Carboxylic Acid-Functionalized Polyesters

The thermal stability of the functional polyesters was investigated next using thermogravimetric analysis. The degradation temperature of the acid functional polyesters is somewhat lower than that of the alkene functional precursor polymer, as demonstrated in the TGA curves (Figure 20), which is due to the presence of the carboxylic acid groups that may undergo condensation and decarboxylation when heated. However, the percentage of carboxylic acid side groups has no effect on the thermal stability of the polymers. Overall, all the newly obtained carboxylic acid-functionalized polymers are stable up to approximately 250 ℃ and can be safely heated up to this temperature without any deterioration.

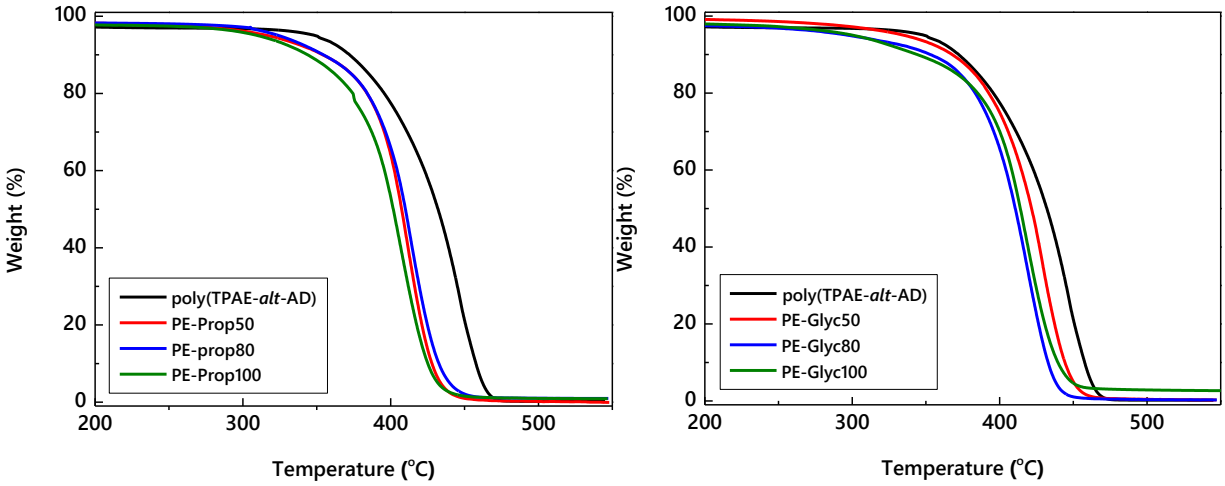

Figure 20: TGA curves of the PE-PropXX (left) and PE-GlycXX (right) polyesters.

The investigation of the thermal properties was also concluded using DSC. In the DSC curves we can only observe the presence of a distinct glass transition temperature (Tg) which indicates amorphous polymers. The precursor polyester shows the lowest Tg than all the modified polyesters, at -55.9 ℃. The fully carboxylic acid-functionalized polyesters, namely PE-Prop100 and PE-Glyc100 show the highest Tg at -36.5 and -26.0 ℃, respectively. Comparing the PE-Prop and the PE-Glyc polymers we observe a slight increase in Tg from the PE-Prop to the PE-Glyc for the 50% carboxylic acid functionalization. Moreover, as the degree of modification increases from 50, to 80 and 100%, the difference in Tg between the PE-Prop and the PE-Glyc also increases, from 2.3, to 4.3 and 10.5 ℃, respectively. Overall, both polyesters show a similar thermal behavior, that is, when the degree of functionalization increases the Tg increases too, which is attributed to the presence of the carboxylic acid groups and the hydrogen bonds formed between the chains that can influence their rigidity and consequently the thermal properties of the polymers.

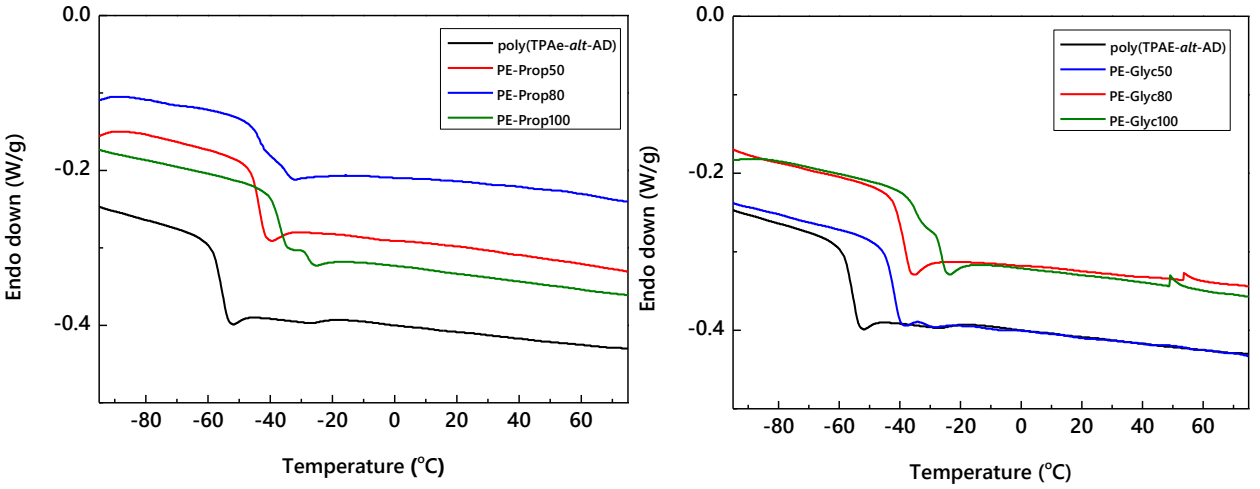

Figure 21: DSC curves of the PE-PropXX (left) and PE-GlycXX (right) polyesters.

Table 5: Thermal properties of the polyesters.

Polyester	Decomposition Temperature (℃)	Glass Transition Temperature (℃)
poly(TPAE-*alt*-AD)	447	-55.9
PE-Prop50	410	-44.0
PE-Prop80	414	-43.3
PE-Prop100	406	-36.5
PE-Glyc50	428	-41.7
PE-Glyc80	418	-39.0
PE-Glyc100	419	-26.0

3.4 Characterization of the pH-Responsive Polyesters in Aqueous Solution

First, the aqueous solution behavior of the pH-sensitive polyesters was examined, by potentiometric titrations. The titration curves (Figure 22) exhibit a plateau region at pH ~ 7 for PE-PropXX and pH ~ 6 for PE-GlycXX. Additionally, the plateau region increases with the degree of modification of the polymers' vinyl groups, suggesting that the carboxylic acid side groups engage in the acid-base equilibrium in this region.

Next, the degree of ionization (α) of the polymer, was calculated from the data derived by the potentiometric titration curves. α was calculated, in the range $0 < \alpha < 1$, as the net uptake of H^+ ions by the carboxylate anions, assuming that all the H^+ from the administered HCl are uptaken by the polymer groups. Figure 23 illustrates the pH for the PE-PropXX and PE-GlycXX polymers as a function of the degree of ionization of the carboxylic acid groups and corresponds to the plateau region of the potentiometric titration curves. Concerning the PE-Prop polyesters, PE-Prop50 and PE-Prop80 are fully ionized at pH 9.0 and fully protonated at pH 4.8, whereas PE-Prop100 is 100% ionized at pH 8.6 and not ionized at pH 4.4. Likewise, PE-Glyc50 and PE-Glyc80 are fully ionized at pH 8.5 and not ionized at pH 4.2, while PE-Glyc100 is 100% ionized at pH 7.8 and not ionized at pH 3.6. The pH at 50% ionization of the weak acid groups is defined as the pK_α, which corresponds to $\alpha = 0.5$. As shown in Table 6, the effective pK_α values of the acidic groups for

PEProp100 increased from 6.6 to 6.9 for PE-Prop50 and PE-Prop80. Compared to the pK_α value of 3-mercaptopropionic acid at 4.3, there is a significant difference.

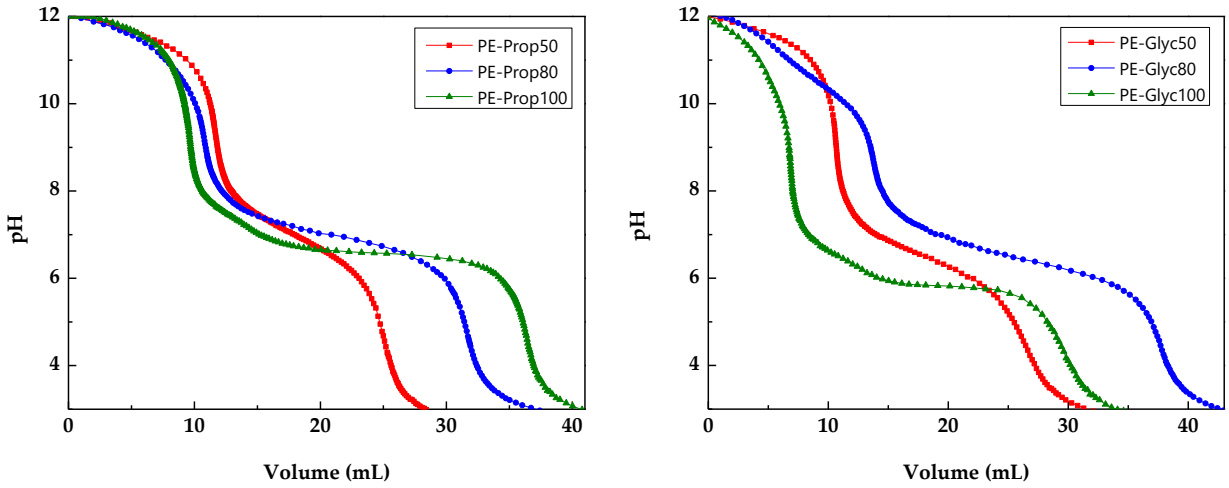

Figure 22: Potentiometric titration curves of the PE-PropXX (left) and PE-GlycXX (right) polyesters.

This difference is related to both the hydrophobicity of the polymer and the polyelectrolyte effect, which cause the dielectric constant to decrease and the Coulumbic interactions to intensify, thus inhibiting the ionization of the carboxylic acid side groups of the polymers. The presence of non-modified alkene side groups in PE-Prop50 and PE-Prop80 enhanced the hydrophobicity of the copolymer even more, resulting in higher effective pK_α values. Similarly, for the PE-Glyc polyesters, the effective pK_α value of the acidic groups for PE-Glyc100 was found at 5.8 and increased to 6.4 for PE-Glyc50 and 6.5 for PE-Glyc80 (Figure 23 and Table 6). As discussed above, because of the polyelectrolyte effect and the hydrophobicity of the polymers, these values are greater than the pK_α of thioglycolic acid at 3.8 and increase even further for PE-Glyc50 and PE-Glyc80 which bear hydrophobic alkene side groups. Furthermore, the effective pK_α values for all the PE-GlycXX polyesters were lower than those reported for their PE-PropXX counterparts, a difference that becomes more notable for the fully modified polyesters, and it is due to the shorter alkyl chain length of the polymer side groups, glycolic vs. propionic, which led to the reduction in the hydrophobicity of the polymers and promoted the ionization of the acidic moieties. Even

though, the pK_α values of the synthesized polyesters ranged from 5.8 to 6.9, enabling the development of new pH-sensitive polymers with the required pK_α value, by appropriately adjusting the hydrophobicity/hydrophilicity of the polymer side groups.

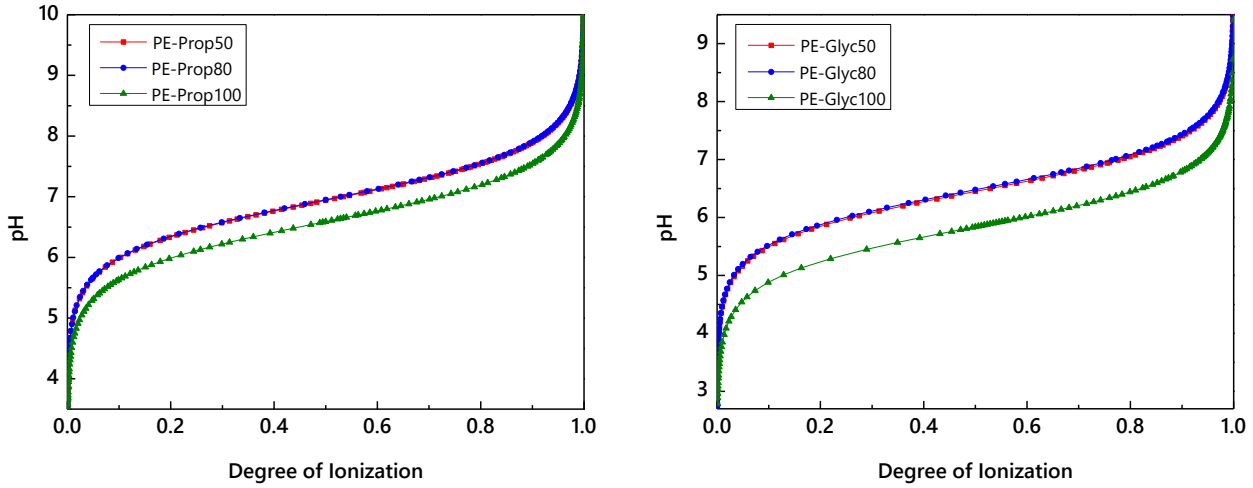

Figure 23: Potentiometric titration data plotted as the pH *vs* the degree of ionization ($0 < a < 1$) of the carboxylic acid side groups for the PE-PropXX (left) and PE-GlycXX (right) polyesters.

The protonation/deprotonation process of the pendant carboxylic acid groups can also alter the polymer solubility in water. For this purpose, turbidimetry measurements were used to evaluate the pH-responsive behavior of the carboxylic acid functionalized polyesters. More specifically, the transmittance of dilute aqueous polymer solutions at λ = 650 nm was measured as a function of the solution pH, at room temperature (Figure 24), in order to obtain the transition pH, which is the pH at which the polymer solution turns turbid.

As shown in Figure 24, PE-Prop50 exhibited a sharp transition in its transmittance at pH 8.1, suggesting that the polymer is soluble at high pH values but becomes hydrophobic at lower pH values. This transition is shifted to pH 7.2 and to pH 6.7 for PE-Prop80 and PE-Prop100, respectively, indicating that as the content of the carboxylic acid side groups in the copolymer increases, the copolymer becomes more hydrophilic, as expected. Taking into account the degree

of ionization of the acid groups as a function of the solution pH, shown in Figure 23, PE-Prop50 is only soluble in water when 93% of the acidic side groups are ionized, and it becomes insoluble as the degree of ionization reduces. Similarly, the degree of ionization at the transition pH for PE-Prop80 was found at ~67% and for PE-Prop100 at ~51%, suggesting that as the content of carboxylic acid side groups increases, the degree of ionization required to solubilize the polymer decreases. In all cases, the aforementioned degrees of ionization at the transition pH is equal to approximately 50 ionized monomer repeat units, indicating that, despite the rise in the content of the carboxylic acid pendant groups on the polymer chains, the ionized carboxylic acid units required to dissolve polymers in water remains relatively constant.

PE-Glyc polyesters showed a similar pH-responsive behavior. At pH 6.9, PE-Glyc50 exhibited a phase transition, corresponding to a 71% degree of ionization, whereas PE-Glyc80 at pH 6.4 (degree of ionization 44%) and PE-Glyc100 at pH 5.6 (degree of ionization 37%). Likewise, the degree of modification of the alkene side groups reduces the transition pH, suggesting that as the content of the carboxylic acid pendant groups increases, the hydrophilicity of the copolymer increases too. As already observed above, the number of ionized monomer repeat units required to solubilize the polymers remains relatively constant at about 36 units, while the degree of ionization at the transition pH is decreasing for PE-Glyc50, PEGlyc80, and PE-Glyc100. Comparing the PE-GlycXX and PE-PropXX copolymers at the same degree modification, it is observed that the transition pH, as well as the degree of ionization, at the transition pH is lower for the PE-GlycXX copolymers, suggesting their higher hydrophilicity, which is attributed to the shorter alkyl chain length of the functional pendant groups.

Table 6: Characterization data of the pH-responsive polyesters.

Polyester	**Degree of Modification**	**pK_α**	**Transition pH**
PE-Prop50	49	6.9	8.1
PE-Prop80	83	6.9	7.2
PE-Prop100	100	6.6	6.7
PE-Glyc50	46	6.4	6.9
PE-Glyc80	83	6.5	6.4
PE-Glyc100	100	5.8	5.6

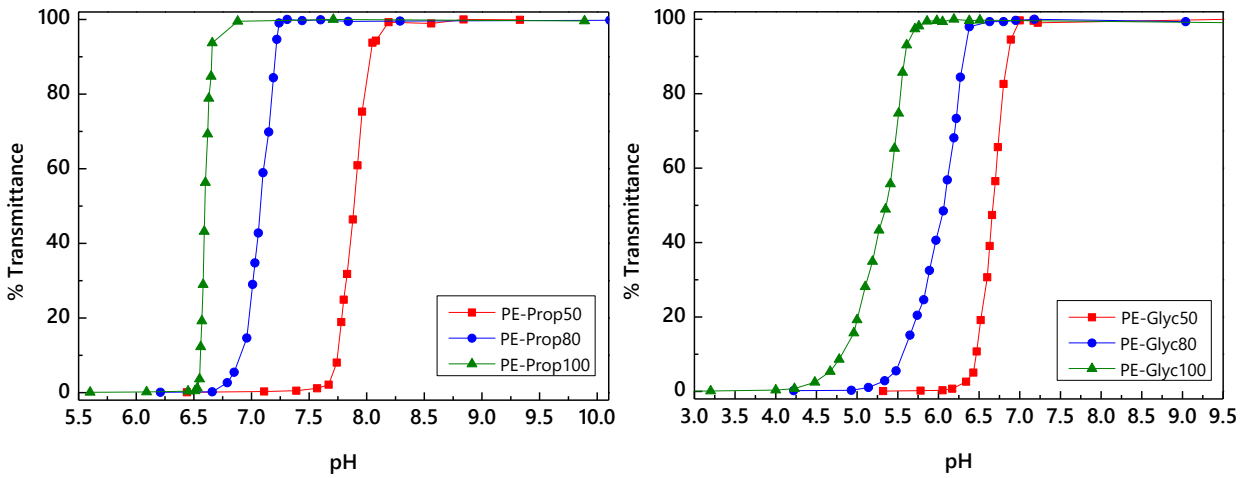

Figure 24: Transmittance of dilute aqueous solutions of the PE-PropXX (left) and PE-GlycXX (right) polyesters as a function of the solution pH.

3.5 Deposition of Thin Polyester Films on Glass Substrates

The produced functional polyesters that combine carboxylic acid and alkene side groups are considered especially appealing as materials for the preparation of pH-responsive polyester-based crosslinked polymers and films. Thus, thin polymer films coated on glass coverslips were used to evaluate the biological characteristics of the produced functional polyesters. For the thin film preparation, initially the coverslips were modified with MAPTMS (Scheme 3, 1st step), in order to functionalize them with polymerizable methacrylate groups, which were next utilized to chemically link the polyester films on the substrate by coupling them with the vinyl bonds present along the polyester backbone, and thus enhancing the adhesion and stability of the films. A solution of the polymer in $CHCl_3$, also containing DMPA as the photoinitiator, was drop-casted and subsequently spin-coated onto the pre-silanized glass substrates. The thin films were irradiated for 90 min, to promote polymer crosslinking and chemical bonding to the substrates (Scheme 3, 2nd step). In the absence of any vinyl side-groups, PE-Prop100 and PE-Glyc100 could not form films onto the substrates. Profilometry was used to measure the thickness of the dry crosslinked films which was found between 100–200 nm for all copolymer samples.

1st Step: Glass substrate silanization

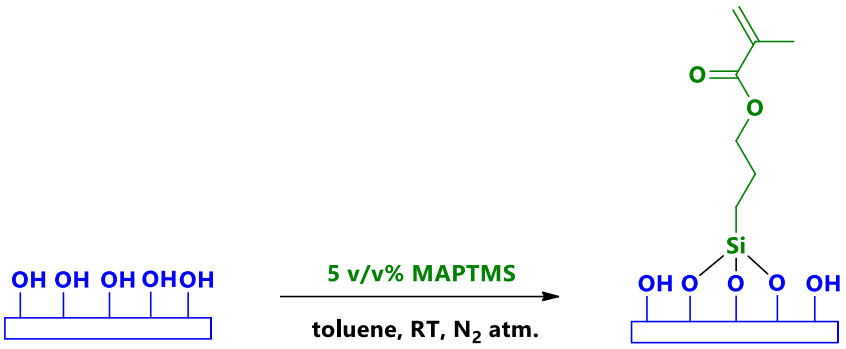

2nd Step: (A) Crosslinked poly(TPAE-*alt*-AC) films

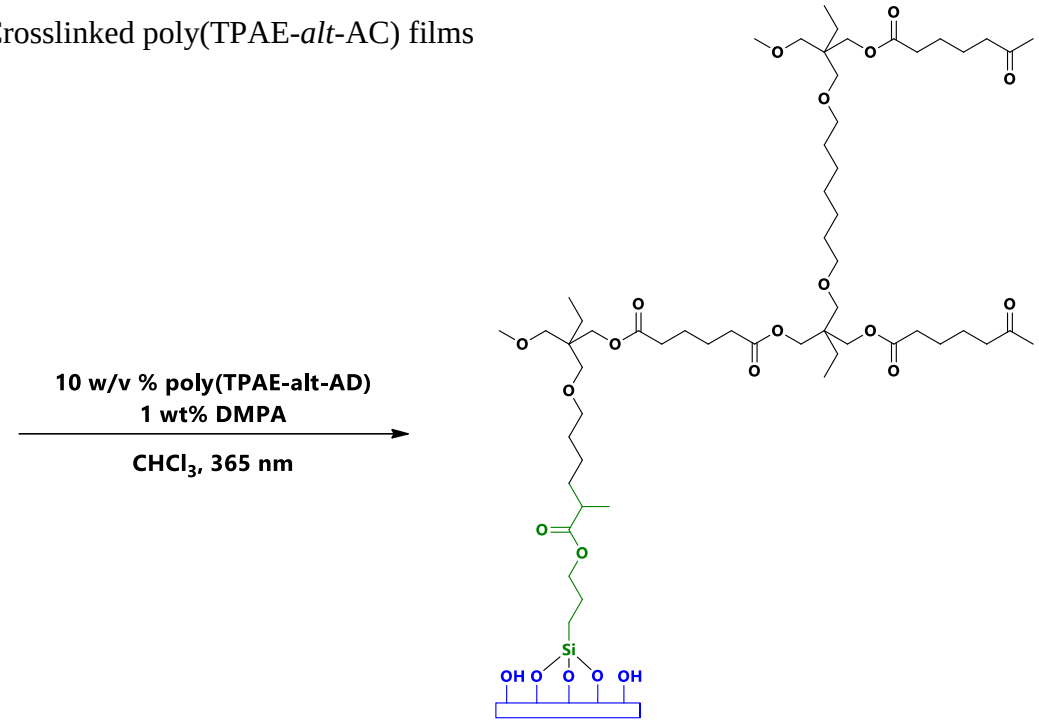

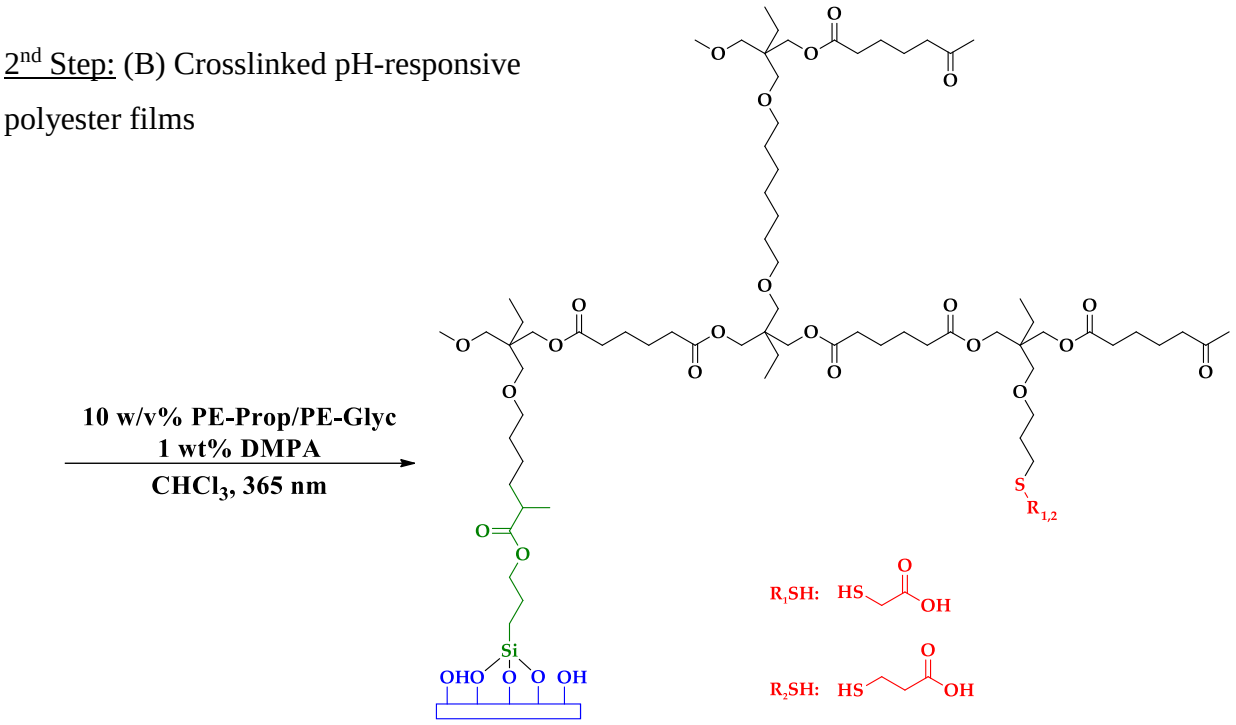

Scheme 3: Schematic representation of the synthetic procedure followed for the preparation of the polyester films.

3.6 Assessment of the Wettability of the Thin Polyester Films

The hydrophilicity of a material surface is an essential property that influences its biological performance, such as cell adhesion and proliferation. Therefore, static WCA was used to investigate the wettability of the crosslinked polyester films and to determine the effect of the degree of modification of the polyester, on the hydrophilicity of the polymer surface. As shown on Table 7, the wettability was found similar for almost all the modified films with a WCA of ~85°, which is also similar to the WCA of the alkene functional precursor polyester. Only the PE-Glyc80 film was found more hydrophilic than the rest, with a WCA of 75°. These findings indicate that by changing the polymer to bear carboxylic acid side groups does not change significantly the wettability of the films. According to these findings, to enhance the hydrophilicity of the polymer surface, it is necessary to have both a shorter alkyl chain side group and a higher content of ionizable carboxylic acid pendant moieties.

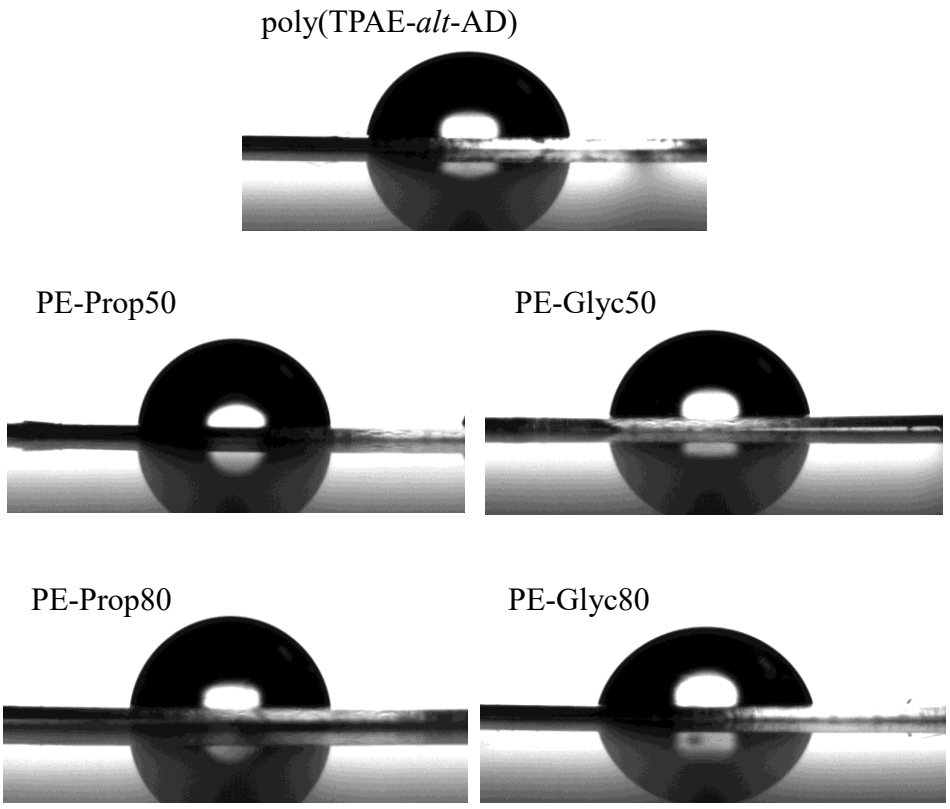

Figure 25: Static water contact angles on crosslinked thin films

Table 7: WCAs on thin polyester films.

Polyester	**Water Contact Angle (°)**
poly(TPAE-*alt*-AD)	83±1
PE-Prop50	86±1
PE-Prop80	84±1
PE-Glyc50	83±1
PE-Glyc80	75±1

3.7 Adhesion and Morphology of Fibroblasts Cultured onto the Polyester Films

The cell adhesion and morphology of L929 fibroblasts on the crosslinked polyester thin films, were assessed by inverse optical microscopy and were compared to the TCPS control after 4 days in culture. As demonstrated at Figure 26, the poly(TPAE-*alt*-AD) and the PE-Prop50 films showed a very low cell adhesion, with the few adherent cells appearing stressed and round, implying that these materials do to promote cell adhesion, viability, and proliferation. The PE-Glyc50 film demonstrated a moderate number of adherent cells which was decreased compared to the TCPS control, however they showed good cell adhesion. Finally, both substrates with the 80% carboxylic acid-functionalized polyesters showed the best cell adhesion, compared to the TCPS control, with the PE-Glyc80 demonstrating a dense cell population with extended pseudopodia as compared to all other surfaces including the TCPS control, whereas the PE-Prop80 showed a similar cell adhesion to the TCPS control both in terms of morphology and number.

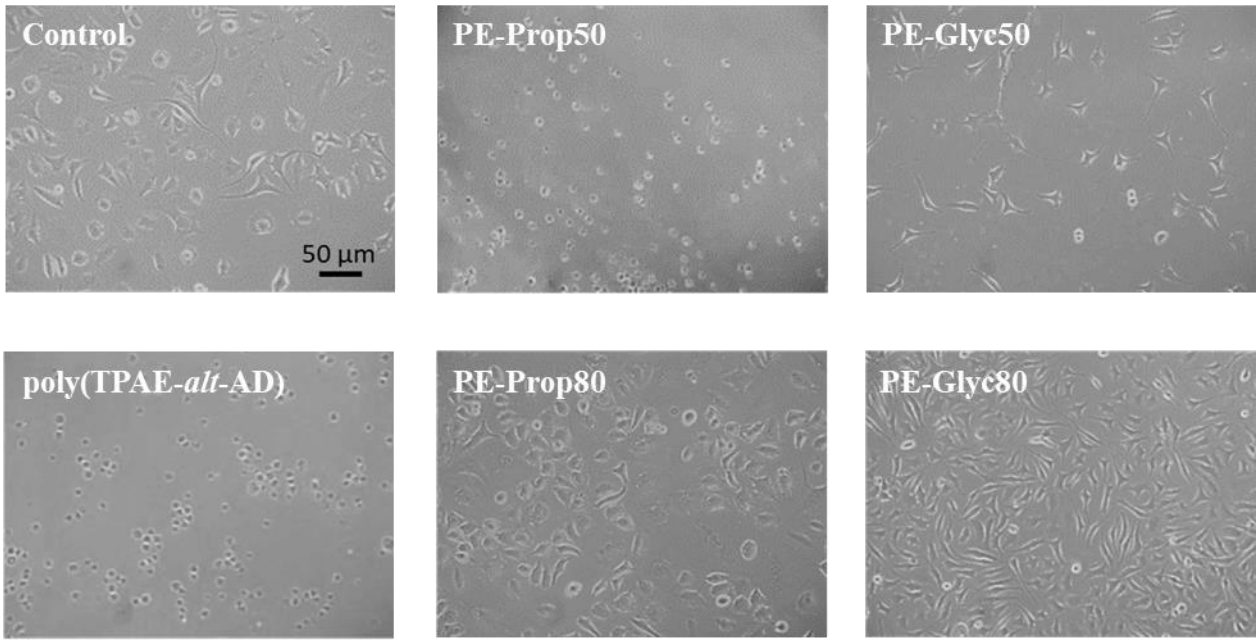

Figure 26: Optical microscopy images depicting the adhesion and morphology of L929 fibroblasts on the polyester films after 4 days in culture.

3.8 Evaluation of the Cell Viability and Proliferation on the Polyester Films

For the evaluation of the cell viability and proliferation on the polyester thin films after 2, 4 and 7 days in culture, the cell viability assay with PrestoBlue™ was used. The results shown in Figure 27, are displayed as absorbance values at 570/600 nm and as percent viability, in comparison with the control TCPS substrate. On day 2, the precursor polyester poly(TPAE-*alt*-AD), as well as the 50% carboxylic acid-functionalized polyesters, PE-Prop50 and PE-Glyc50, presented significantly ($p < 0.05$) lower cell viability compared to the TCPS control, whereas the PE-Prop80 and PE-Glyc80 films showed better results, with the latter slightly exceeding the TCPS control, without statistical significance. Similarly, on day 4, the PE-Glyc80 demonstrated a statistically significant increase ($p < 0.01$) compared to the TCPS control substrate. Eventually, on day 7, the same trend was followed, with the PE-Glyc80 and PE-Prop80 substrates favoring the cell viability, with the former exceeding the control substrate, and reaching 128%, and the latter reaching 80% of the viability of the TCPS surface. These findings show that the polyester with the shorter alkyl chain length and the highest fraction of carboxylic acid groups, PE-Glyc80, exhibited a maximum cell survival, even better than the positive control substrate.

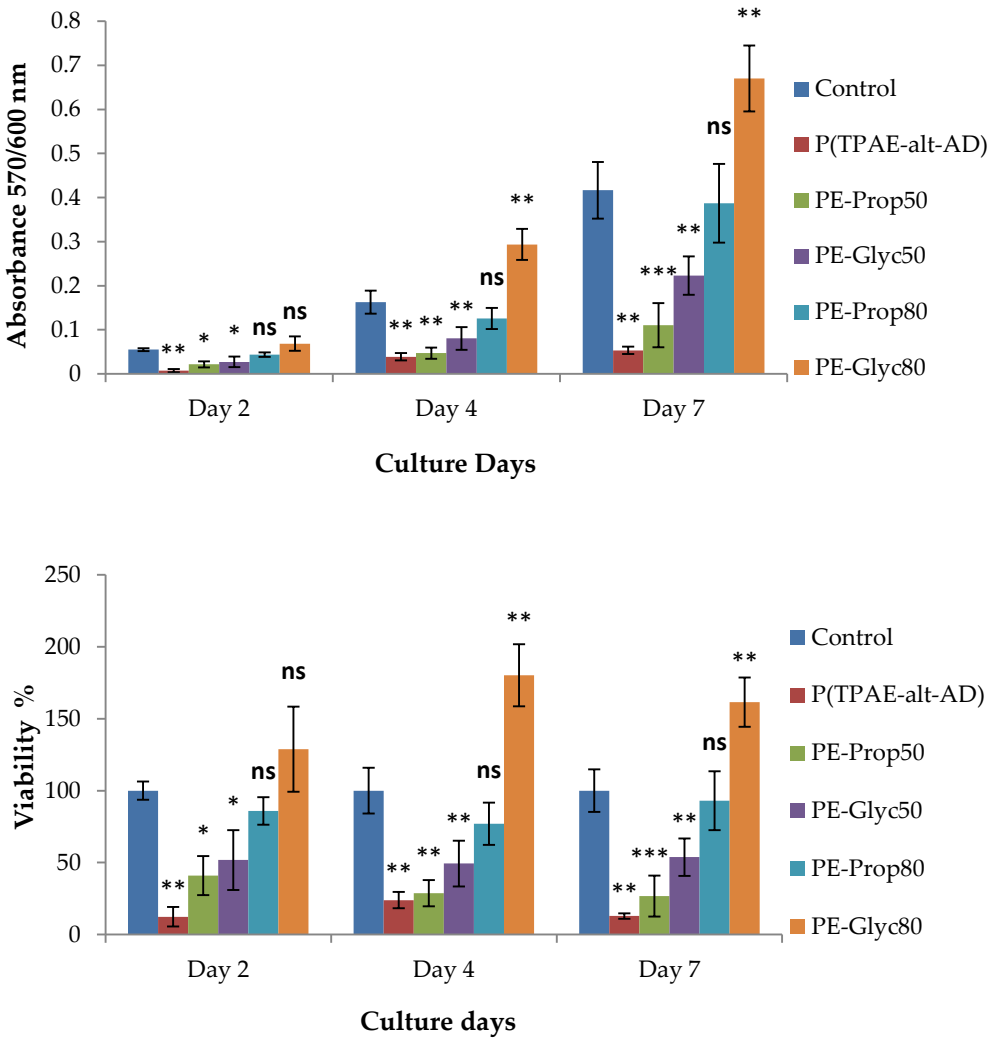

Figure 27: Cell viability and proliferation showing the absorbance at 570/600 nm (top) and the % viability (bottom) compared to the TCPS control on the functional polyester films at days 2, 4 and 7.

3.9 3D printing of pH-Responsive Polyester and Polyester/Laponite Hydrogels

As already mentioned above, one of the major components of TE are bioactive biomaterial scaffolds that can imitate and replace real tissues. To this end, the carboxylic acid-functionalized polyester with the optimum cell viability results, PE-Glyc80, was used to develop 3D-printing materials via an extrusion-based method.

The PE-Glyc80 polyester is a viscous, “honey-like” fluid that has poor printing properties. The first approach to improve the printing fidelity of the material, was to blend it with the same silane used for the thin film preparation. In this method, the polyester was blended with MAPTMS, at different v/v% concentrations, and DMPA as the photoinitiator, and was subsequently heated at 80 ℃ for 1 h, under vacuum, to induce the hydrolysis and condensation of the silane (Scheme 4). Next, the blend was loaded in a syringe, in order to evaluate its printability. The extrusion was performed under UV irradiation (λ = 365 nm) and all tests resulted in a dropwise flow from the syringe needle. In a slightly different procedure, the same blend was UV-cured before the extrusion through the needle, which resulted in a solid glass-like material, which could not be extruded.

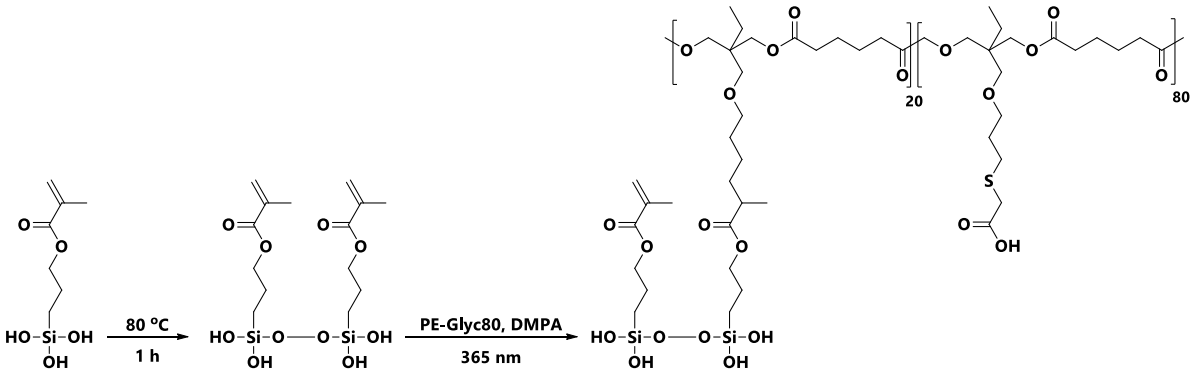

Scheme 4: Schematic representation of the PE/MAPTMS ink.

The second approach included the introduction of a photosensitive crosslinker that would have the ability to react with the remaining alkene groups and would transform the viscous polyester into a soft printable material. For this purpose, DL-dithiothreitol (DTT) was used as the crosslinker because it is a dithiol and could thus be coupled to the alkene groups of the polyester via a thiol-ene click reaction (Scheme 5). The polyester was blended with DTT and DMPA and was UV-cured, while being extruded from the nozzle. The blend was also UV-irradiated prior to extrusion to investigate its potential to solidify. The results using DTT as the cross-linker were similar to those obtained with MAPTMS.

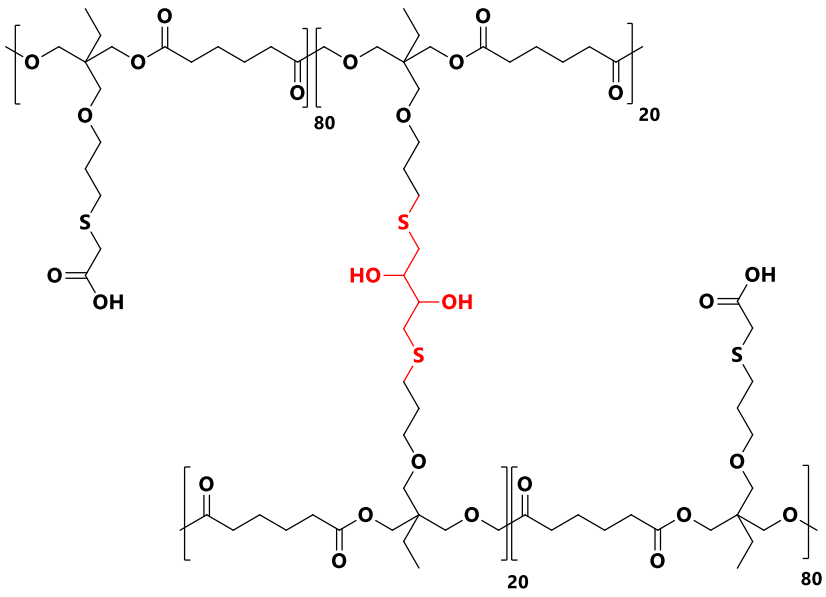

Scheme 5: Schematic representation of the PE-Glyc80/DTT ink.

In out next approach we used poly(ethylene glycol) dimethacrylate with an average M_n = 750 g/mol (PEGDMA 750) as a more efficient crosslinker. PEG has been used previously in 3D-printing applications[35]. Similar to DTT, PEGDMA 750 was used as a crosslinker to chemically bind its methacrylic groups with the vinyl groups of the polyester (Scheme 6). To this end, PE-Glyc80/85, PEGDMA 750 and DMPA were blended and were then irradiated with UV light, resulting in soft hydrogels. After several trials and optimization, the ideal hydrogel, with shear thinning properties and continuous shape-maintaining flow, was obtained with the 80% glycolic acid-modified polyester at a 1:1 mole ratio of the alkene groups of the polyester to the PEGDMA 750. The choice of solvent proved also to be very important, since the scaffolds are intended for TE applications. In this case, acetone was selected, as it is a good solvent for the polyester, with a low boiling point (56 ℃) and thus easy to be removed post printing. Acetone was also mixed with deionized water in a 90:10 volume ratio to improve the printability of the hydrogels. Finally, to secure the structures all 3D-printed hydrogels were treated with UV light (Figure 28).

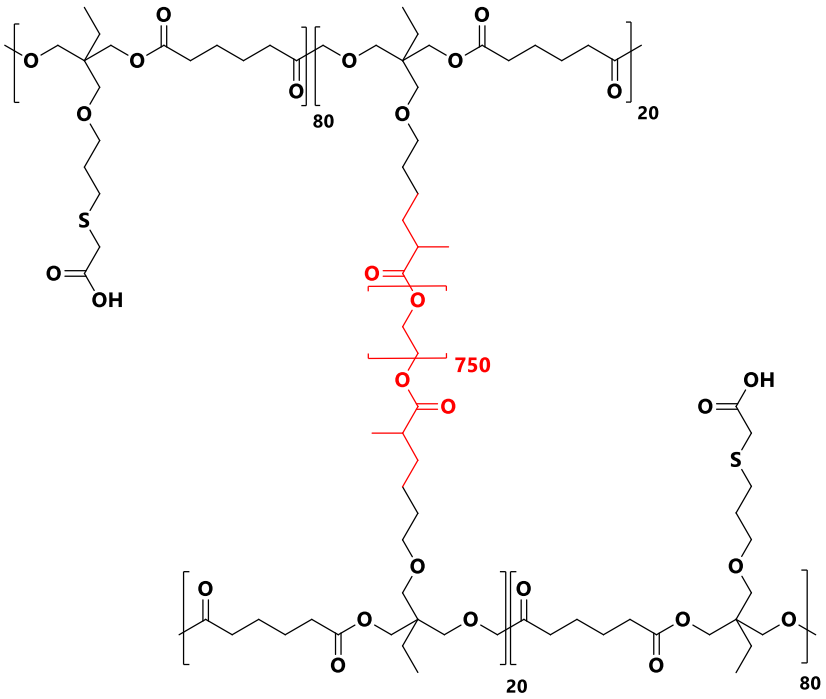

Scheme 6: Schematic representation of the PE-Glyc80/PEGDMA 750 ink.

After the optimization of the printing characteristics of the polyester (PE) hydrogels, a nanoclay, namely laponite, was utilized in the polymer to obtain hybrid polyester/laponite (PE/LAP) structures. Laponite was selected because it has been shown to improve the printing fidelity, act as a crosslinker, and also improve the scaffold's bioactivity by augmenting cell spreading and osteogenesis in TE constructs[36].

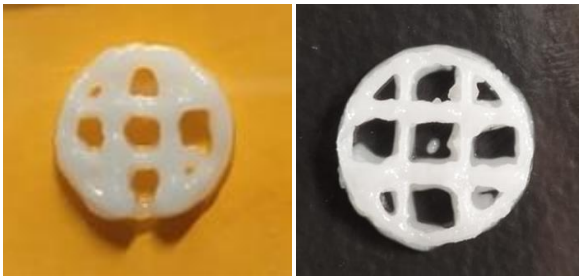

Figure 28: The 3D printed PE hydrogel (left) and PE/LAP hydrogel (right).

3.10 Thermal Stability of the PE and PE/Laponite Hydrogels

Next, the thermal stability of the polyester and polyester/laponite hydrogels was investigated by TGA. As demonstrated by the TGA curves (Figure 29), the materials were stable up to about 200 ℃. When the temperature reached 360 ℃, about 20% of the weight was lost for both hydrogels, which is attributed to the presence of the PEGDMA 750 crosslinker. After this temperature, a sharp decay of the mass of the materials is observed, with the degradation temperature of the PE hydrogel (Td = 414 ℃) being slightly higher compared to that of the PE/Laponite analogue (Td = 390 ℃). As expected, the organic hydrogel decomposes completely, whereas the ~ 12 wt% mass residue is attributed to the inorganic laponite in agreement with the initial mass used for the preparation of the PE/Laponite hydrogels.

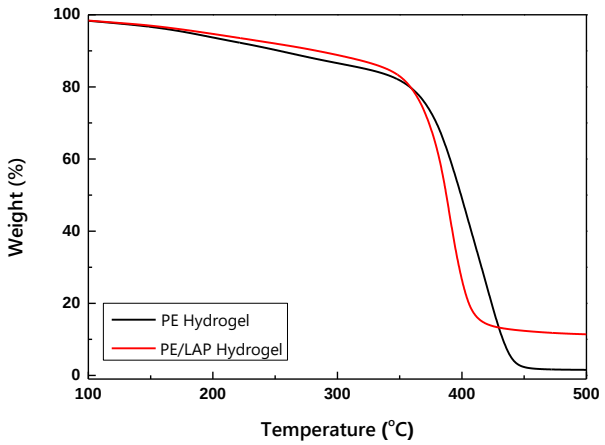

Figure 29: TGA thermographs of the PE and PE/Laponite hydrogels.

3.11 Evaluation of the pH-Dependent Behavior of the PE and PE/Laponite Hydrogels

Next, the influence of the solution pH on the hydrogel properties was evaluated. The chosen pH values were pH 3 at which the polyester PE-Glyc80 is fully protonated and insoluble, pH 6.0 which is the pK_{α} of the polyester and pH 9.2 when the polyester is fully deprotonated and water soluble. Finally, pH 7.4 was also examined because it is the body's physiological pH.

Overall, the PE and PE/Laponite hydrogels exhibited a similar swelling behavior (Figure 30). As expected, all samples demonstrated a maximum swelling at alkaline pH (9.2) when the carboxylic acid groups are ionized, due to electrostatic repulsion and the increase of the osmotic pressure within the hydrogels. Lower degrees of swelling were obtained at neutral and acidic pH, due to the deprotonation of the carboxylic acid groups.

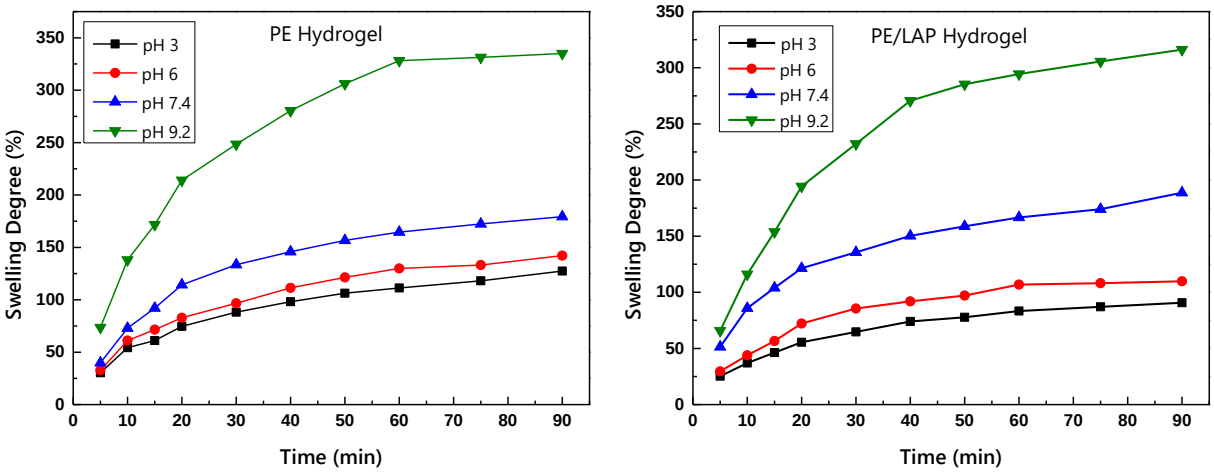

Figure 30: Swelling profile of the PE and PE/Laponite hydrogels at different pH values.

SEM was used to assess the morphology of the water swollen hydrogels at different pH values. In agreement with the swelling measurements, some porosity was observed for the hydrogels which seemed to increase with the solution pH, however, further and more detailed studies are required to quantify the porosity and pore size of the hydrogels as a function of the solution pH.

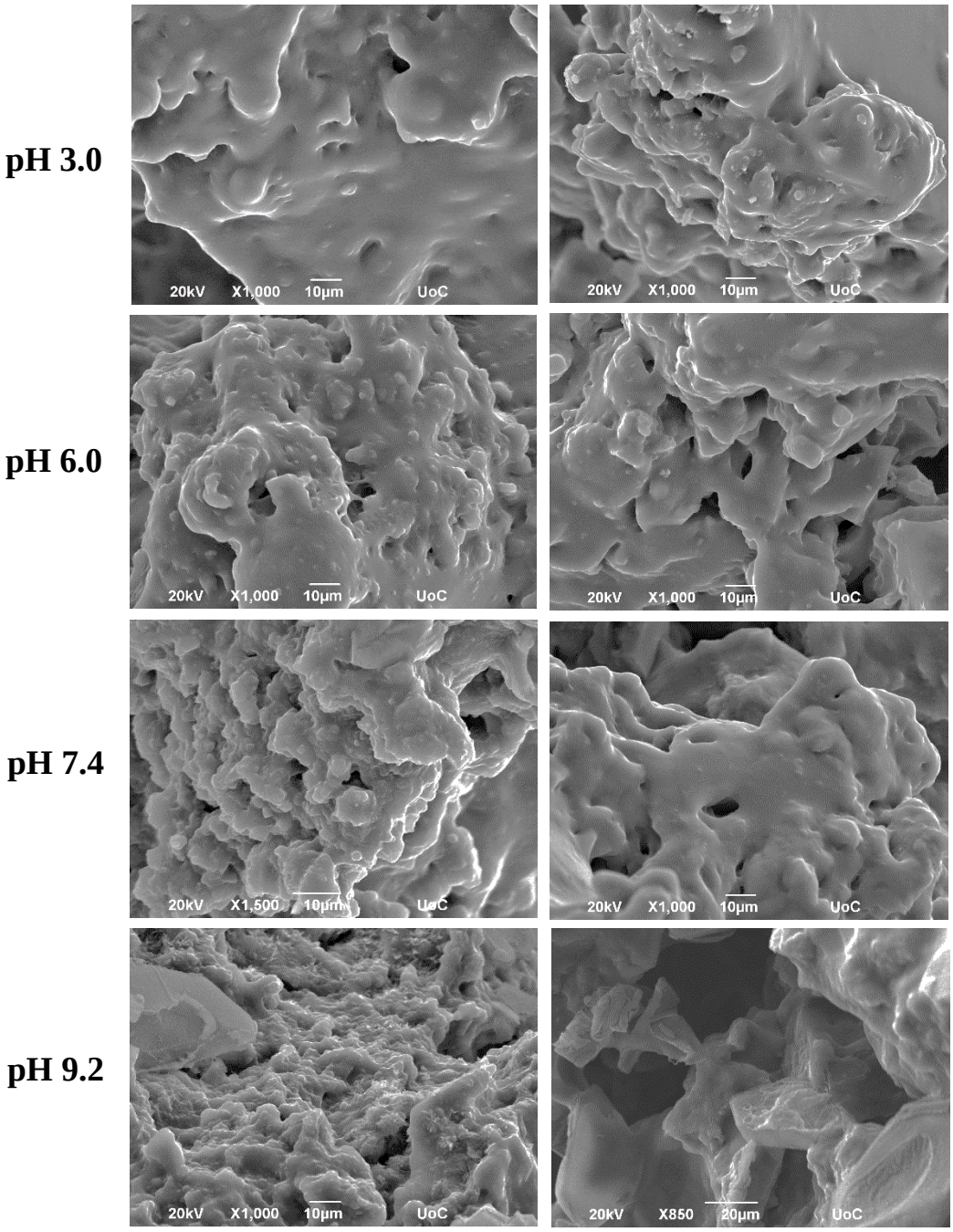

Figure 31: SEM images of the swollen PE (left) and PE/LAP (right) hydrogels.

3.12 Degradation Profile of PE and PE/LAP Hydrogels

Finally, the degradation degree of the synthesized structures was measured. Both hydrogels were investigated in pH 7.4 at 37 ℃, showing a similar degradation degree at around 15% at the first 7 days, where the presence of the laponite does not seem to affect the degradation rate of the hydrogels.

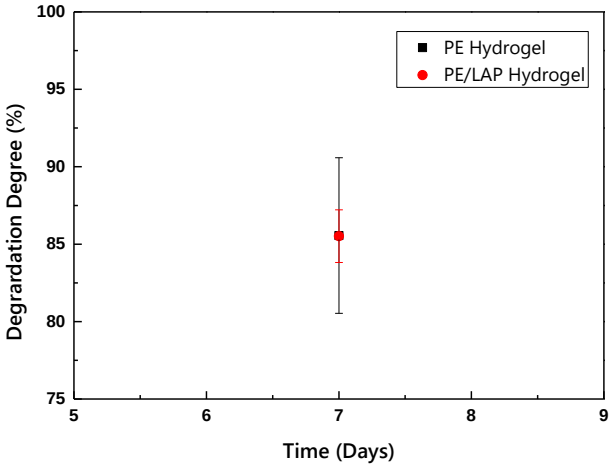

Figure 32: Degradation degree of PE and PE/LAP hydrogels.

Chapter 4

4. Conclusions

In conclusion, aliphatic polyesters with alkene side groups were synthesized by condensation copolymerization of a diol with a diacid chloride. The alkene-bearing polymers were further modified via an optimized photo-induced thiol-ene reaction to bear carboxylic acid pendant groups. For this purpose, two mercaptocarboxylic acids, namely 3-mercaptopropionic and thioglycolic acid, were used to functionalize the precursor polymer with weak acid side groups. Three distinct functional polyesters derived from each type of carboxylic acid, with approximately 50, 80, and 100% carboxylic acid side groups were synthesized, by simply varying the time of irradiation between 40 s to 5 min. All new polyesters were structurally characterized by ^{1}H NMR and ATR-FTIR spectroscopies confirming the successful synthesis, whereas their thermal properties were investigated by TGA and DSC revealing that all the polyesters are amorphous. Next, their responsive behavior was studied by potentiometric titrations and turbidimetry, to correlate the degree of ionization of the acidic side groups and the polymer solubility in aqueous media, with the solution pH. The results showed, polyesters with tunable pK_{α} values and solubility ranging from hydrophobic and water insoluble in acidic pH to hydrophilic and water soluble in alkaline pH. Having established their structural, physicochemical and pH-responsive properties, the materials were used to prepare crosslinked thin polyester films by deposition onto pre-silanized glass substrates followed by UV irradiation to chemically link the pendant alkene functionalities with the substrate. The wettability of the crosslinked functional polyester films was investigated by static WCA measurements showing marginally hydrophobic behavior demonstrated by the 50% functionalized polyesters with the longer alkyl chain length and hydrophilic behavior for the shorter alkyl chain length and the highest degree of modification. Cell viability and proliferation studies on the cross-linked polyester films showed a superior performance of the PE-Glyc80 surface, which promoted the adhesion and growth of L929 fibroblasts to a greater extent compared to the TCPS control surface, verifying an excellent cell behavior on the polymer. Thereafter, PE-Glyc80 was selected for the development of a 3D printable biomaterial. To improve the printing fidelity, the polyester was pre-crosslinked with PEGDMA 750 using UV light, which resulted in a soft, easily extruded hydrogel that was UV-treated to secure the 3D printed structure. To boost the potential bioactivity of the scaffold, laponite, a nanoclay used widely in tissue engineering

applications, was blended with the polyester, and the hybrid material was 3D printed. Both the PE and PE/Laponite 3D scaffolds were evaluated for their thermal properties by TGA and their swelling behavior was investigated as a function of the solution pH, whereas their degradability was investigated in physiological pH. Future work, is currently being conducted, to improve the printing fidelity of the materials, to further explore their degradability through larger periods of time and to investigate the rheological and mechanical properties of the scaffolds, as well as to examine their use as functional, bioactive materials and structures in 3D cell cultures for tissue engineering applications.

5. References

1. Ikada Y. Challenges in tissue engineering. *J R Soc Interface*. 2006;(3):589-601. doi:10.1098/rsif.2006.0124
2. Griffith LG, Naughton G. Tissue Engineering - Current Challenges and Expanding Opportunities. *Science (80-).* 2002;(295):1009-1016. doi:10.1126/science.1069210
3. Caddeo S, Boffito M, Sartori S. Tissue engineering Approaches in the Design of Healthy and Pathological In Vitro Tissue Models. *Front Bioeng Biotechnol*. 2017;5(July):1-22. doi:10.3389/fbioe.2017.00040
4. Babensee JE, Mcintire L V, Mikos AG. Growth Factor Delivery for Tissue Engineering. *Pharm Res*. 2000;17(5):497-504.
5. Amini AR, Laurencin CT, Nukavarapu SP. Bone Tissue Engineering: Recent Advances and Challenges. *Crit Rev Biomed Eng*. 2013;40(5):363-408.
6. Stevens MM. Biomaterials for bone Materials that enhance bone regeneration have a wealth of potential. *Mater Today*. 2008;11(5):18-25. doi:10.1016/S1369-7021(08)70086-5
7. Hubbell JA. Biomaterials in Tissue Engineering. *Biotechnology*. 1995;13(June):565-576.
8. Brien FJO. Biomaterials & Scaffolds for Tissue Engineering. *Mater Today*. 2011;14(3):88-95. doi:10.1016/S1369-7021(11)70058-X
9. Ullah S, Chen X. Fabrication, applications and challenges of natural biomaterials in tissue engineering. *Appl Mater Today*. 2020;20. doi:10.1016/j.apmt.2020.100656
10. Joyce K, Fabra GT, Bozkurt Y, Pandit A. Bioactive potential of natural biomaterials : identification , retention and assessment of biological properties. *Signal Transduct Target Ther*. 2021;6(122):1-28. doi:10.1038/s41392-021-00512-8
11. Huang J, Best SM. Ceramic Biomaterials. In: *Tissue Engineering Using Ceramics and Polymers*. Woodhead Publishing Series in Biomaterials; 2007:3-31. doi:10.1533/B978-1-84569-176-9.50001-0
12. Dolcimascolo A, Calabrese G, Conoci S. Innovative Biomaterials for Tissue Engineering. In: *Biomaterial-Supported Tissue Reconstruction or Regeneration*. ; 2019.
13. Albertsson AC. Aliphatic Polyesters: Synthesis, Properties and Applications. In: *Degradable Aliphatic Polyesters*. Springer, Berlin; 2002:1-40.
14. Kaliva M, Georgopoulou A, Dragatogiannis DA, Charitidis CA, Chatzinikolaidou M, Vamvakaki M. Biodegradable Chitosan- graft -Poly(l -lactide) Copolymers For Bone

Tissue Engineering. *Polymers (Basel)*. 2020;12(2):1-19.

15. Georgopoulou A, Kaliva M, Vamvakaki M, Chatzinikolaidou M. Osteogenic Potential of Pre-Osteoblastic Cells on a Chotosan-graft-Polycaprolactone Copolymer. *Materials (Basel)*. 2018;11(4):1-14. doi:10.3390/ma11040490
16. Seyednejad H, Ghassemi AH, Nostrum CF Van, Vermonden T, Hennink WE. Functional aliphatic polyesters for biomedical and pharmaceutical applications. *J Control Release*. 2011;152(1):168-176. doi:10.1016/j.jconrel.2010.12.016
17. Lee JH, Jung HW, Kang I, Lee HB. Cell behaviour on polymer surfaces with different functional groups. *Biomaterials*. 1994;15(9):705-711.
18. Washington KE, Kularatne RN, Karmegam V, Biewer MC, Stefan MC. Recent advances in aliphatic polyesters for drug delivery applications. *Nanomedicine Bionanotechnol*. 2017;9(4). doi:10.1002/wnan.1446
19. Tong R. New Chemistry in Functional Aliphatic Polyesters. *Ind Eng Chem Res*. 2017;56(15):4207-4219. doi:10.1021/acs.iecr.7b00524
20. Tardy A, Honoré J, Tran J, et al. Radical Copolymerization of Vinyl Ethers and Cyclic Ketene Acetals as a Versatile Platform to Design Functional Polyesters. *Angew Chemie - Int Ed*. 2017;56(52):16515-16520. doi:10.1002/anie.201707043
21. Sampath UG, Chee CY, Chuah CH, Sabariah JJ, Lin P. Fabrication of Porous Materials from Natural/Synthetic Biopolymers and Their Composites. *Materials (Basel)*. 2016;9(991):1-32. doi:10.3390/ma9120991
22. Kačarević ŽP, Rider P, Alkildani S, et al. An introduction to bone tissue engineering. *Int J Artif Organs*. 2019;43(6). doi:10.1177/0391398819876286
23. Rim NG, Shin CS, Shin H. Current approaches to electrospun nanofibers for tissue engineering. *Biomed Mater*. 2013;8(1):014102. doi:10.1088/1748-6041/8/1/014102
24. Bedell ML, Navara AM, Du Y, Zhang S, Mikos AG. Polymeric Systems for Bioprinting. *Chem Rev*. 2019;120(19):10744-10792. doi:10.1021/acs.chemrev.9b00834
25. Foyt DA, Norman MDA, Yu TTL, Gentleman E. Exploiting Advanced Hydrogel Technologies to Address Key Challenges in Exploiting Advanced Hydrogel Technologies to Address Key Challenges in Regenerative Medicine. *Adv Healthc Mater*. 2018;7(8). doi:10.1002/adhm.201700939
26. Ligon SC, Liska R, Stampf J, Gurr M, Mülhaupt R. Polymers for 3D Printing and

Customized Additive Manufacturing. *Chem Rev*. 2017;117(15):10212-10290. doi:10.1021/acs.chemrev.7b00074

27. Chen Z, Zhao D, Liu B, Nian G, Li X, Yin J. 3D Printing of Multifunctional Hydrogels. 2019;1900971:1-8. doi:10.1002/adfm.201900971
28. Li J, Wu C, Chu PK, Gelinsky M. 3D printing of hydrogels : Rational design strategies and emerging biomedical applications. *Mater Sci Eng R*. 2020;140:100543. doi:10.1016/j.mser.2020.100543
29. Hassan A, Crespilho N, Ornelas C. The structure – property relationship in LAPONITE materials : from Wigner glasses to non-covalent interactions. *Soft Matter*. 2019;15:1278-1289. doi:10.1039/c8sm01965g
30. Davila JL, D'Avila MA. Rheological evaluation of Laponite / alginate inks for 3D extrusion-based printing. *Int J Adv Manuf Technol*. 2019;101:675-686.
31. Dong L, Bu Z, Xiong Y, Zhang H, Fang J, Hu H. Facile extrusion 3D printing of gelatine methacrylate / Laponite nanocomposite hydrogel with high concentration nanoclay for bone tissue regeneration. *Int J Biol Macromol*. 2021;188(August):72-81. doi:10.1016/j.ijbiomac.2021.07.199
32. Ausili A, Sanchez M, Gomez-Fernandez J. Attenuated total reflectance infrared spectroscopy : A powerful method for the simultaneous study of structure and spatial orientation of lipids and membrane proteins. *Biomed Spectrosc Imaging*. 2015;(4):159-170. doi:10.3233/BSI-150104
33. Gill P, Moghadam TT, Ranjbar B. Differential Scanning Calorimetry Techniques: Applications in Biology and Nanoscience. *J Biomol Tech*. 2010;21(4):167-193.
34. Yan Y, Siegwart DJ. Scalable synthesis and derivation of functional polyesters bearing ene and epoxide side chains. *Polym Chem*. 2014;(5):1362-1371. doi:10.1039/c3py01474f
35. Rutz AL, Hyland KE, Jakus AE, Burghardt WR, Shah RN. A Multimaterial Bioink Method for 3D Printing Tunable, Cell-Compatible Hydrogels. *Adv Healthc Mater*. 2015:1607-1614. doi:10.1002/adma.201405076
36. Ahlfeld T, Cidonio G, Kilian D, et al. Development of a clay based bioink for 3D cell printing for skeletal application. *Biofabrication*. 2017;9(034103).

37. https://www.wikidoc.org/index.php/File:SizeExChrom.jpg

38. https://microbenotes.com/nuclear-magnetic-resonance-nmr-spectroscopy/
39. https://www.sciencedirect.com/science/article/pii/B9780323461399000049
40. https://www.netzsch-thermal-analysis.com/en/products-solutions/differential-scanning-calorimetry/dsc-214-polyma/
41. https://en.wikipedia.org/wiki/Tissue_engineering#/media/File:Tissue_Engineering.png
42. https://www.smacgigworld.com/blog/principle-uv-vis-spectroscopy-.php
43. https://www.nanoscience.com/techniques/tensiometry/
44. https://www.researchgate.net/publication/330541768_Liquefaction_mitigation_with_nano particles